Research and Development on Critical (Sonic) Flow of Multiphase Fluids through Wellbores in Support of Worst-Case-Discharge Analysis for Offshore Wells

**Mewbourne School of Petroleum and
Geological Engineering
The University of Oklahoma, Norman
100 E Boyd St. Norman, OK-73019**

The UNIVERSITY of OKLAHOMA

May 30, 2018

This page intentionally left blank.

Research and Development on Critical (Sonic) Flow of Multiphase Fluids through Wellbores in Support of Worst-Case-Discharge Analysis for Offshore Wells

Authors:

Saeed Salehi, Principal Investigator
Ramadan Ahmed, Co- Principal Investigator
Rida Elgaddafi, Postdoctoral Associate
Olawale Fajemidupe, Postdoctoral Associate
Raj Kiran, Research Assistant

This page intentionally left blank.

DISCLAIMER

Table of Contents

List of Figures

List of Tables

Nomenclature

Abbreviations and Acronyms

A	Cross-section area of the test section
BOEM	Bureau of Ocean Energy Management
BOP	Blowout Preventer
BPV	Bypass valve
BSEE	Bureau of Safety and Environment Enforcement
CSB	Chemical Safety Board
CO	Compressor
CV	Check valve
D	Diameter
DAQ	Data acquisition
DP	Differential pressure
f	Fanning friction factor
f_D	Darcy friction factor
g	Gravitational acceleration
GoM	Gulf of Mexico
HPHT	High-pressure high-temperature
gpm	Gallon per minute
H_L	Liquid holdup
H_T	Total height of the test section
HV	Holdup valve
ID	Inner diameter
L	Distance between pressure transducer ports
LOWC	Loss of Well Control
Ma	Mach number
OD	Outer diameter
PDF	Probability density function
PSD	Power spectral density
Pwf	Bottomhole pressure
QL	Volumetric liquid flow rate
Q_G	Mass flow rate of the gas
Re	Reynolds number
V	Mean fluid velocity
VFD	Variable frequency drive
V_{LSP}	Single phase liquid velocity
V_L	Liquid volume
Vsl	Liquid superficial velocity
Vsg	Gas superficial velocity

V_T	Total volume of the test section
WCD	Worst Case Discharge
WCTC	Well Construction Technology Centre
$\left(\frac{\Delta P}{L}\right)_t$	Total pressure gradient
$\left(\frac{\Delta P}{L}\right)_h$	Hydrostatic component of pressure gradient
$\left(\frac{\Delta P}{L}\right)_a$	Acceleration component of the pressure gradient
$\left(\frac{\Delta P}{L}\right)_f$	Friction component of the pressure gradient

Greek Symbols

ϵ	Roughness height
ρ	Fluid density
ρ_l	Density of the liquid phase

Executive Summary

This report presents an experimental study carried out at the University of Oklahoma under BSEE/BOEM project no. M16PS00059. The report presents: i) outcomes of a literature survey on experimental studies of two-phase pipe and annular flows; and ii) experimental setup and results. The first part of this report discusses factors that can influence worst case discharge (WCD) and the reasons it should be investigated. The second section presents results of past experimental studies on multiphase flow performed in pipes and annuli. The report describes the test setup and instrumentation employed to carry out experimental studies in vertical pipe and annulus, and presents measurements and analysis of results and interpretations.

This study aims to investigate flow parameters such as pressure gradient, flow patterns, and liquid holdup at high Mach number of two-phase flow, which may influence worst case discharge (WCD). These parameters are investigated in vertical pipe and annulus. Understanding these factors at high Mach number, a mechanistic model can be developed to predict WCD accurately. Most of the existing models employed in predicting WCD are not accurate. This is because the models are based on measurements obtained at low Mach number flows.

Before the experimental investigation, gas-liquid flow in vertical pipe and annulus were carefully reviewed to develop a test plan. Experiments were carried out varying gas and liquid velocities. Pressure gradient, pressure profile in the test sections, and liquid holdup were measured. Visual observation and recorded videos were employed to identify flow regime. The liquid holdup was measured using quick closing valves installed at inlet and outlet of the test sections. Pressure gradient measurements were obtained from two pressure transducers that are installed close to the exit of the test sections.

Some of low gas superficial velocity measurements are compared with published studies. The measurements demonstrated good agreement with results of other studies. However, the results deviated from published measurements at high superficial gas velocities.

1. Introduction

1.1. Background

Worst case discharge (WCD) resulting from a blowout has been a major concern in oil and gas industry. During drilling operations, an uncontrolled release of fluids from the reservoir into the well-bore, known as blowout may occur. The consequences of such an event can be physical injury/death to rig personnel, contamination of the environment, and to clean up the spill can cost the company a fortune. The main aim of installing (BOP), which is well control equipment, is to prevent the discharge of hydrocarbon fluids from the oil and gas well into an operational environment. The principal functional mechanism of BOP is to close the annular space between drilling pipe and casing when a kick is detected. However, BOP may fail to function during a kick incident and as a result of the failure, uncontrolled amount of reservoir fluid will be released into the operational environment.

Reservoir fluid exist beneath the earth under high-pressure high-temperature (HPHT) condition, therefore most of the gas is dissolved in the liquid hydrocarbon. The solution gas is released out of the liquid hydrocarbon as the pressure and temperature are reduced as the reservoir fluid approaches the well-bore and become multiphase flow. Therefore, if the reservoir fluid migrates after influx, the hydrocarbon is transported upward as multiphase flow within the annulus/pipe. Due to a gradual reduction in pressure, as the fluid travels upward in the annulus/pipe, the solution gas evolves and expands rapidly, pushing the liquid phase to the surface vigorously. However, there are other factors such as liquid holdup, flow regimes, pressure losses which affect this phenomenon. Therefore, experimental investigations are needed to examine the contribution of each of the factor. Several studies have carried out at low superficial gas velocities using different diameter vertical pipes measuring liquid holdup and pressure loss. However, gas-liquid flows at high superficial gas velocities (subsonic and supersonic) have never been explored.

1.2. Objectives

The objectives of this study are to:

1. Improve understanding of the impact of high Mach number (0.3 – 1+ Mach) flow on WCD calculation.
2. Identify and investigate flow patterns (churn, annular, and mist) and flow geometry variation (casing and/or tubing).
3. Investigate two-phase flow behavior in vertical pipe and annulus at high superficial gas velocities.
4. Develop an experimental database to formulate a robust two-phase flow model.

2. Literature Review

2.1. Previous Incidents of Blowouts

The systemic flaws during Deep-water Horizon incident have brought a lot of discussion on the in-situ parameters and operation of the offshore oil rigs. According to the U.S. Chemical Safety Board (CSB), Volume 2, identifying safety-critical elements and tasks ensure that safety barriers and controls are essential parameters in dealing with the complex systems (CSB report, 2014). In addition, taking a closer look at the theoretical and technical aspects can reveal several gaps in the understanding and limitations of the existing theories and models, which are used without taking into considerations the actual flow conditions in the wellbore. Loss of well control (LOWC) incidents has existed in oil and gas operations since its inception. Loss of well control can be defined as the uncontrolled flow of formation or other fluids which may be to an exposed formation (underground blowout) or at the surface (surface blowout) or flow through a diverter or uncontrolled flow resulting from a failure of surface equipment or procedures" (Per Holland, 2017). The LOWC incidents can be classified into blowouts (surface and underground), well release, and diverted well release.

Petroleum industry has been experiencing incidents of blowouts since 1964 (Baker Drill Barge). **Table 2.1** depicts blowouts incidents that occurred in past decades (Bourgoyne et al., 1995; CSB report, 2016). Shortly, after the Macondo incident several measures have been taken to reduce blowouts incidents. However these unfortunate situations have not been completely eradicated. For instance, in the US GoM, 2013 Hercules 265 blowout, the BOP failed to close during high flow, and after 13 hours of the uncontrolled flow of natural gas, there was fire on the rig (Per Holland, 2017). These incidents only point out at the vulnerability of current theoretical understanding and technological limitations. Therefore, it is necessary to improve the current system and the conceptual understanding of these undesirable incidents to ensure a safe oil and gas drilling operations in the future.

Table 2.1 Blowout incidents and location

Year	Location	Incident	No People Killed
1964	Gulf of Mexico,	Baker drill barge	22
1969	Gulf of Mexico	Submersible Tideland	-
1972	Gulf of Mexico	Jackup Storm II	-
1975	Gulf of Mexico	Jackup Storm II	-
1979	Gulf of Mexico	Jackup SalenergyII	-
1980	Gulf of Mexico	Jackup Ocean King	5
1988	North Sea	Ocean Odyssey Semi-	1
2007	Gulf of Mexico	Usumancita Jackup	22
2009	Nigeria	KS Endeavour	-
2009	North Sea	Sedco 711	
2009	North Sea	Gullfaks	-
2010	Gulf of Mexico	Deepwater Horizon	11
2011	South America	Frade	-
2012	North Sea	Elgin	-
2013	Offshore Louisana	Hercules	-

2.2. Worst Case Discharge

Blowout incidents lead to the discharge of a considerable volume of crude oil into the nearby affected zones and release enormous amount of gas into the atmosphere. It was disclosed in the current report prepared for BSEE, that 58 blowout incidents occurred in US Gulf of Mexico and 36 from another part of the world have occurred between 2000 to 2015 (Per Holand, 2017). Some of the major oil and condensate spills as a result of blowouts published by Per Holand, 2017 are presented in **Table 2.2**.

Table 2.2 Amount of crude oil spilled during major blowouts (Per Holand 2017)

Country	Amount of Crude Oil discharge (bbl)
Montara, Australia	29000
Macondo, USA	4250000
Frade, Brazil	3700

According to Per Holand (2017), Macondo blowout spill was 140 times greater than the Montara blowout and 1,150 times larger than the Frade blowout in terms of amount of oil released. Oil spills pose a major question about the existing fail-safe system. Limitations of the current predictive models and insufficient design envelope of the onsite equipment have been attributed to the system failure. Finally, lack of an appropriate model for the estimation of worst-case discharge constrains the design and regulatory work. In the early occurrence of the Macondo incident, some guidelines were established by the Bureau of Ocean Energy Management (BOEM) for the estimation of Worst Case Discharge (WCD) for the improvement of wellbore safety (Bowman, 2012; Moyer et al., 2012). Worst case discharge was defined by (BOEM) as the daily rate of an uncontrolled flow from all producing reservoirs into the open wellbore. This incorporates all hydrocarbon-bearing zones in each open-hole section as it is planned to be drilled. The uncontrolled flow is considered as casings and liner that are not obstructed, and absence of drill pipe in the hole. Based on the uncontrolled flow at the sea floor with a hydrostatic water head or atmospheric pressure at sea level with well work on an existing platform WCD rates for deep-water wells are calculated. For such unexpected events, efforts have been made some years back to predict the flow conditions accurately and calculate operational parameters. Nevertheless, these calculations were based on flow models which were not developed for the calculation of WCD in extreme conditions. Actually, the probability that WCD will occur is low. However, it can be experienced while drilling. In an event where drilling margin is insufficient, over-pressurized formations penetrated during well construction, this leads to an influx of formation fluid in the annulus at small scale, and can lead to uncontrolled fluid flow and WCD.

Over-pressurized formations can occur naturally or be created as a result of injection of water or gas in the nearby wells. The WCD rates differ among oil and gas wells based on reservoir inflow and wellbore outflow parameters and can be implemented in risk assessment process. Accurate prediction of WCD rate, proper designing of the system and holistic monitoring of the operation will prevent such scenario to occur. The most important of such scenario is WCD rate

15

predictions; the significant step is to establish the building blocks. Worst Case Discharge estimation depends on many parameters that account for reservoir inflow and wellbore outflow. Reservoir parameters (such as permeability, porosity, pressure, and temperature) in inflow model and wellbore characteristics (such as depth, flow pattern, phase velocity, geometry) in outflow model play a significant role. Fluid movement in reservoir formation is mainly impacted by permeability and porosity of a formation, and these parameters governed the rate of influx from the formation. The bottom hole pressure and temperature set a differential condition and provides a driving force to the fluid to flow from bottom to the surface of the wellbore. Temperature increase tends to cause thermal expansion of wellbore fluids in sealed annuli and can worsen the flow issues (Oudeman and Kerem, 2006). The depth of oil and gas wells has a significant influence on the pressure gradient inside the annulus and thus affects the discharge rate.

Multiphase flow characteristics such as phase velocity, flow patterns, and geometry will also influence WCD. Multiphase flow is a common occurrence in oil and gas operations. This fluid dynamics problem leads to the question of understanding the mechanisms behind the multiphase flow system. The efforts to understand and characterize the intricacies of flow started with the development of empirical correlations and with time-shifted towards mathematical modeling and simulation approach. Statistical analysis and interpretation of experimental results are used to develop empirical correlation and mechanistic models. The mechanistic approach is developed based on the understanding of the mechanism and developing mathematical representations of the process using governing equations with the imposed boundary conditions. The hypothesis of every approach is dependent on flow patterns or flow configurations. Then, it becomes essential to answer that which model most closely replicates the in-situ phenomenon. On this subject, a lot of confusions and disagreements exist. Several models have been developed to better understand two-phase flows; nevertheless, each model has its own limitations. Due to this reason, the models cannot explain the full complexity of the flow occurring in reality. Most of the time, experimentalist disagrees with theoreticians: the experimentalists claim that empirical models provide reasonable prediction than the theoretical models while theoreticians stress that theoretical models provide better prediction than the empirical models for a wide range of field conditions, which cannot be replicated in a laboratory experiment. The theoretical models are defined based on the physics of the flow. However, their development involves some assumptions and simplifications. Hence, it is highly desirable to look into the details of the problem and find common ground between these two approaches. Besides in-situ conditions, the time dependence of the flow also influences the WCD rate. A steady-state condition refers to the case in which flow characteristics are not changing with time and do not include the real-time input. On the other hand, a transient condition means the flow characteristics varying with time. In harsh well control scenarios, the transient approach is more realistic which can effectively mimic the in-situ dynamic pressure and temperature and allows defining the control sequence for the occurrence within the operational limitations. The discharge rate is affected by the characteristics of reservoir such as pressure, temperature, its drive mechanisms, completion type, wellbore geometry, and production history (Replogle, 2009).

In petroleum industry WCD rate is estimated by using several models such as Beggs and Brill, (1973); Duns and Ros, (1963); Hasan and Kabir, (2007). Well inflow characteristics are evaluated by the model which is based on nodal analysis and incorporate parameters such as permeability, porosity, pressure, and temperature. However, the model is limited due to its steady-state assumption. Other models including empirical, analytical, mechanistic, and numerical are used in wellbore outflow as a complementary to inflow model for WCD rate predictions.

In the post Macondo era, the estimation of WCD rate was mostly evaluated based on simple experimental data and generic models that do not state the severe conditions as stipulated by the regulatory bodies. Accurate prediction of WCD conditions require the development of high Mach number of multiphase flow models which has not been investigated. The Mach number is a dimensionless quantity and can be described as the ratio of flow velocity to the speed of sound in a surrounding medium. Mach number 1 depicts the speed of the sound. However, existing predictive WCD multiphase flow models are developed for low Mach number (i.e., $Ma < 0.1$). For the regulatory bodies and current field conditions requirements to be met, the predictive WCD multiphase models need to be developed, tested, and upgraded for high Mach number and other existing limitations that need to be corrected.

2.3. Flow Regimes in Two-phase Vertical Pipe and Annulus

The studies of gas-liquid flow in pipes over decades were done through classification of flow structure known as flow regimes or flow patterns. Each gas-liquid flow can exhibit one of many different flow patterns, which depend on the flow conditions.

Based on the geometry of the interfaces, Hewitt and Hall-Taylor (1970) categorized gas-liquid multiphase flow regime in vertical upward pipe as bubbly, slug, churn and annular flow. Similarly, (Weisman et al., 1979; Taitel et al., 1980; and McQuillan and Whalley, 1985) reported the same observation in their studies. In bubble flow, the gas phase is dispersed as a discrete bubble in the continuous liquid phase. The flow regime occurs at low gas velocities and upward movement of the small bubbles follows a zigzag path due to slippage between the gas and the liquid phases. The increase of gas flow rate changes the pattern of the flow to slug which is characterized by bullet-shaped bubbles formed as a result of the coalescence of dispersed bubbles and follows by liquid slug body, which bridges the entire cross-sectional area of the pipe and contains small spherical distributed gas bubbles. The bullet-shaped bubbles are called Taylor bubbles. Churn flow occurs at higher gas flows and causes Taylors bubbles to break down thereby destroying the bridging across liquid slugs. The subsequent gas movement sweeps the liquid upward thereby resulting into oscillatory liquid flow. At high gas velocity, the liquid flows on the wall of the pipe, and the gas phase with small liquid droplet flows in the center, this flow regime is called annular.

Study of gas-liquid flow in annulus pipe by Caetano et al. (1992a) showed that flow patterns are similar to those observed in vertical pipes. However, slug and annular flow are different due to the inner tubing in the annulus. The slug flow in annulus exhibits a distorted Taylor bubble with

rising velocity faster than that observed in pipes. Moreover, annular flow existed as two liquid films in the annulus. One of the liquid films flows around the tubing while the other on the casing (Caetano et al., 1992a). This is different from what is observed in the pipe. The flow structures of gas-liquid flow in the vertical pipe or annulus are shown in **Figures 2.1a** and **b**.

(a)   (b)
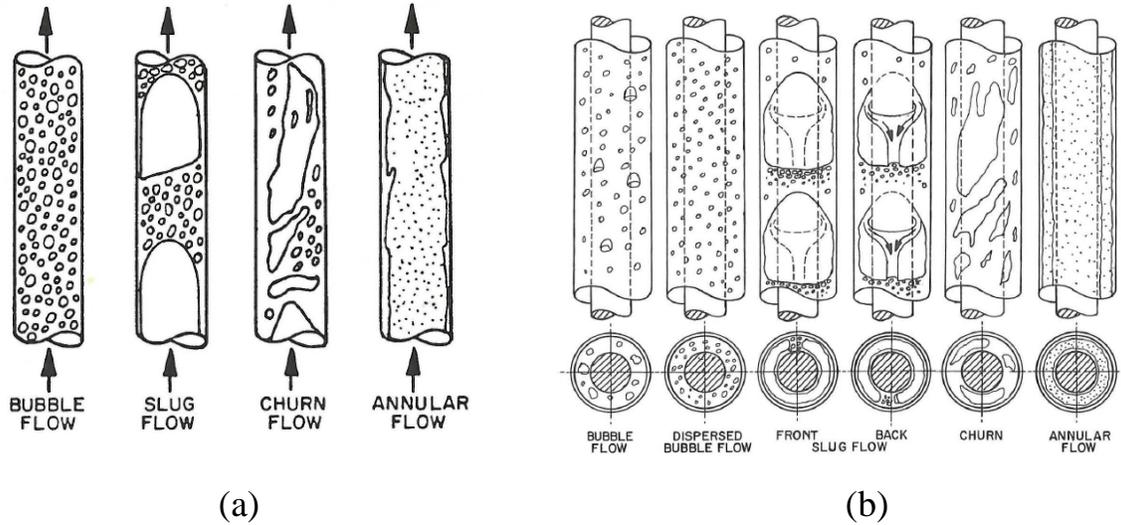
Figure 2.1 Flow pattern in gas-liquid two-phase (a) pipe (b) annulus (Caetano, 1985)

2.4. Flow Regime Identification using Probability Density Function (PDF)

Historically, classification of two-flow patterns is usually determined by visual observation or analysis of recorded video of flow structures during experiments using transparent pipes. Furthermore, flow patterns can also be identified in pipes by measuring and estimating flow variables such as gas void fractions (Barnea et al., 1980; Vince and Lahey, 1982; Costigan and Whalley, 1997; and Tsoukalas et al., 1997). However, a number of studies identified flow regimes by employing probability density function (PDF) or power spectral density (PSD), especially in the case of invisibility of flow through the test section (Jones and Zuber, 1975; Tutu, 1982; Matsui, 1984; and Matsui, 1986). These methodologies make use of peaks and shape characteristics of PDFs or PSDs of measured void fractions or differential time traces. For instance, mist, annular and bubbly flow are identified with PDF of single peak associated with different variance. The single-peaked frequency distribution of a mist flow nears unity while single peak of bubbly flow patterns is sharp. However, slug flow has PDF of differential pressure fluctuation distribution with twin peaks of large variance. The twin peaks are due to high void value of a Taylor bubble and low void value is caused by the passing of the liquid slug body. Probability Density Function of different flow regimes in vertical pipes are shown in **Figure 2.2**.
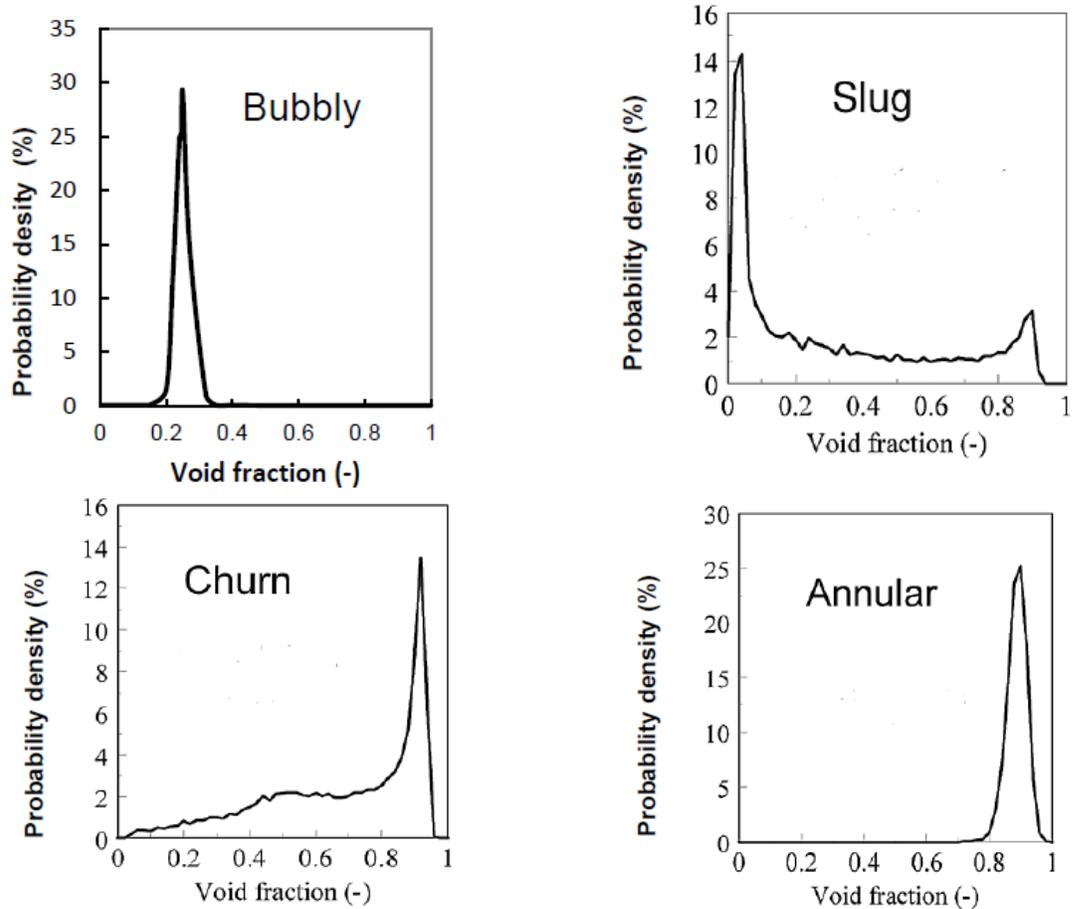
Figure 2.2 Probability density function in vertical pipe (Aliyu, 2015)

2.5. Flow Regime Map

Flow regime map is a graphical representation of gas-liquid flow in pipes. It can be classified into theoretical and empirical (Lixin et al., 2008). Empirical flow pattern maps are generated by fitting them to the observed database while a theoretical flow pattern map predicts transitions of flows from physical models. There are many flow pattern maps for gas-liquid upward flow in vertical pipe developed using different formats. In some studies, flow rates and superficial velocities of the phases were employed as the coordinates (Griffith and Wallis, 1961; Hewitt and Hall-Taylor, 1970; Taitel and Dukler, 1980; Griffith, 1984; and Waltrich et al., 2015). However, some used mass flux (Hewitt and Roberts, 1969). Dimensionless numbers such as gas velocity number (RN) and liquid velocity number (N) are also employed to generate flow regime map (Duns and Ros, 1963). Flow regimes map can also be modified. Caetano (1985) modified Taitel and Dukler (1980) flow regime map for annulus. One of the problems associated with flow regimes map is, most of the flow regime maps are only valid for a specific set of condition or fluids. Some of the flow regime maps in the literature are shown in **Figures 2.3 - 2.6**.
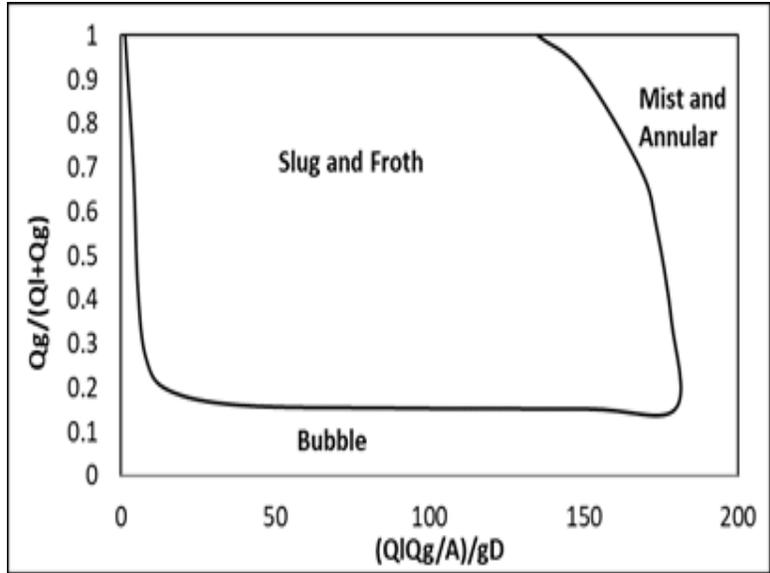
Figure 2.3 Griffith and Wallis (1961) flow regime map
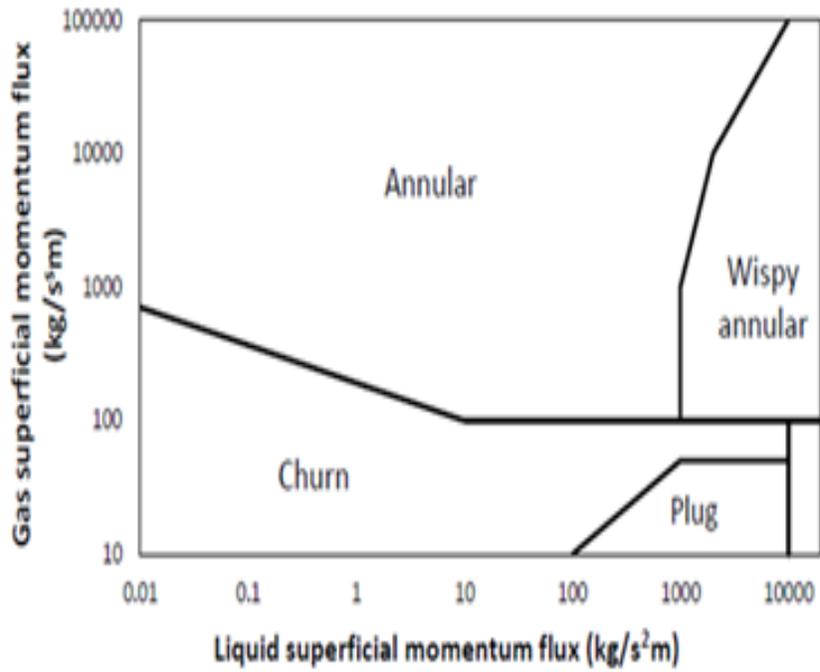
Figure 2.4 Hewitt and Roberts (1969) flow regime map
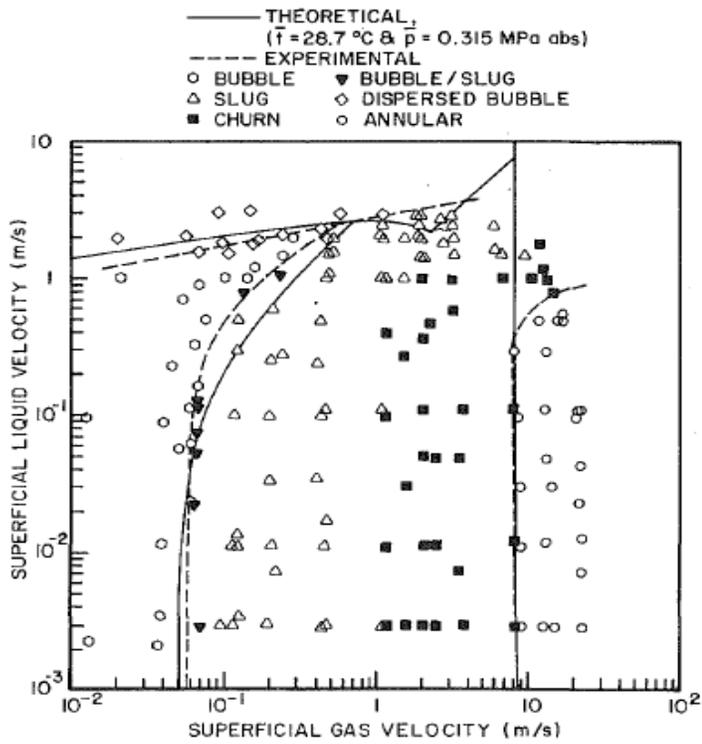
Figure 2.5 Flow regime map (Caetano, 1985)
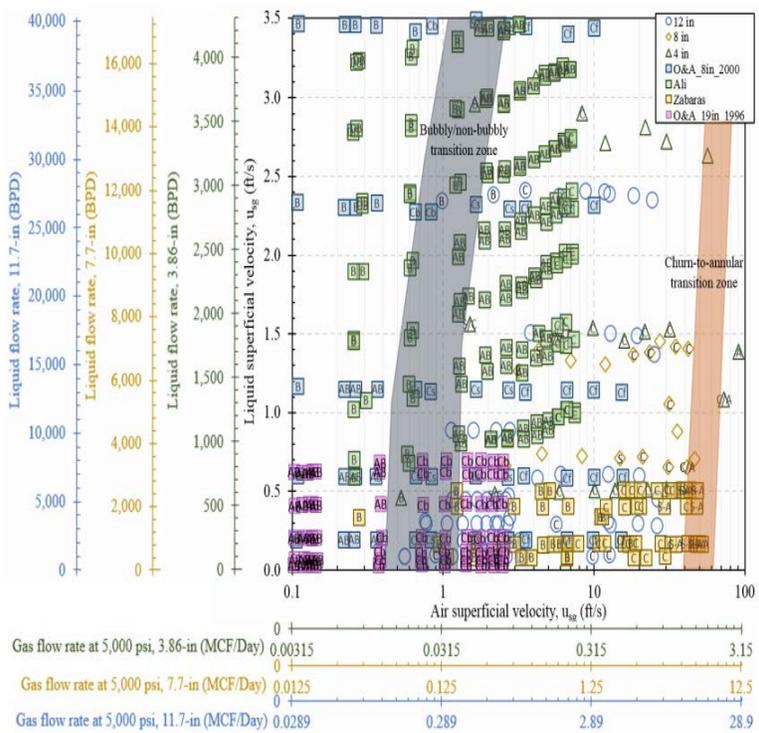
Figure 2.6 Flow regime map (Waltrich et al., 2015)

21

2.6. Multiphase Flow in Vertical Pipes

This section reviews experimental studies of gas-liquid flow conducted in vertical pipe. In general, the multiphase flow phenomenon in the vertical pipe have been experimentally investigated in small (ID < 0.15 m) and large (ID > 0.15 m) pipes diameter. During the experimental studies, the essential parameters such as void fraction, volumetric holdup, pressure drop, and flow patterns are measured. However, only few studies disclosed raw experimental data on these important parameters. One of the important characteristics in the study of multiphase flow is pressure drop along the pipe. In addition, in pipeline design, pressure drop is one of the major parameters needs to be put into consideration. Knowing the amount of pressure drop provides a better understanding of the pumping power needed to transport fluids through pipelines. Several studies (Owen, 1986; and Sawai et al., 2004) linked variation pressure drop with superficial gas velocity to flow patterns and their transition. Variation of time-average pressure gradients with gas superficial velocity (J_g) for various liquid superficial velocity (J_l) is shown in **Figure 2.7**. Sawai et al. (2004) explained that when liquid superficial is very low, pressure gradient characteristics can be classified into four regions. The regions are two negative regions (NS-I and II), and two positive (PS-I and II). When these regions were compared with the flow pattern maps developed by Hewitt and Roberts (1969), the variation of slope against gas superficial velocity correspond to the flow pattern transition.
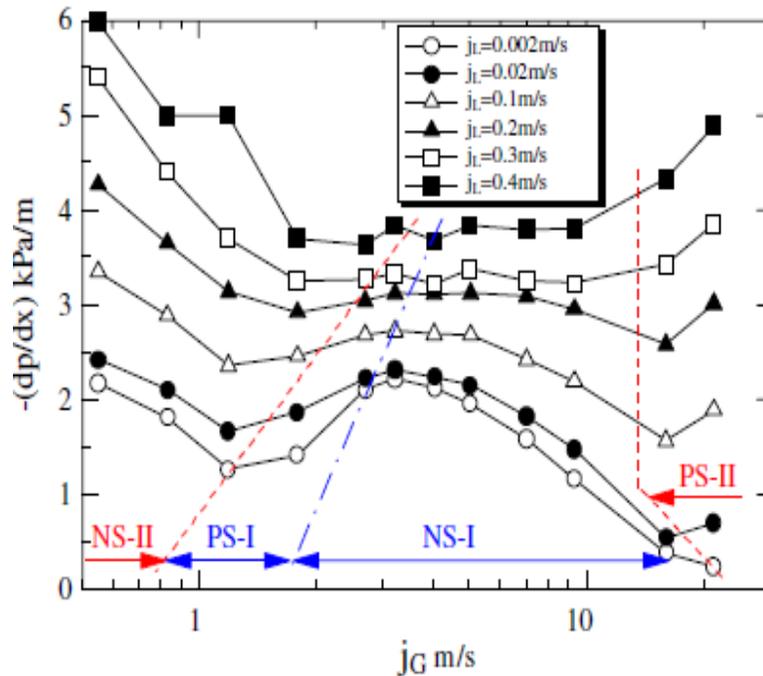
Figure 2.7 Variation of pressure gradient with gas velocity (Sawai et al., 2004)

22

The pressure drop for gas-liquid flow per unit length of a pipe consists of hydrostatic, acceleration and frictional components as shown in Equation 2.1.

$$\left(\frac{\Delta P}{L}\right)_t = \left(\frac{\Delta P}{L}\right)_h + \left(\frac{\Delta P}{L}\right)_a + \left(\frac{\Delta P}{L}\right)_f \qquad\qquad (2.1)$$

where $\left(\frac{\Delta P}{L}\right)_t$ is the total pressure gradient, $\left(\frac{\Delta P}{L}\right)_h$ denotes hydrostatic component, $\left(\frac{\Delta P}{L}\right)_a$ is acceleration component and $\left(\frac{\Delta P}{L}\right)_f$ signifies friction component of the pressure gradient.

The hydrostatic component of two-phase pressure drop represents the effective density of the mixture and the influence of the gravity. Accurate prediction of the void fraction can be employed to estimate hydrostatic component. The acceleration component of pressure drop is usually small and can be neglected in comparison to the hydrostatic and frictional component for short pipe lengths. If the acceleration and frictional components of the total pressure gradient are negligible, the gravitational component dominates the total pressure drop.

The plot of the pressure gradient against gas superficial velocity at fixed liquid superficial velocity is represented in **Figure 2.8**. As the gas superficial velocity increases, the gravitational component of the total pressure decreases. This is due to a reduced liquid holdup at high gas flow rates. Nevertheless, as the gas flow rate increases, the frictional component of the total pressure gradient becomes larger.
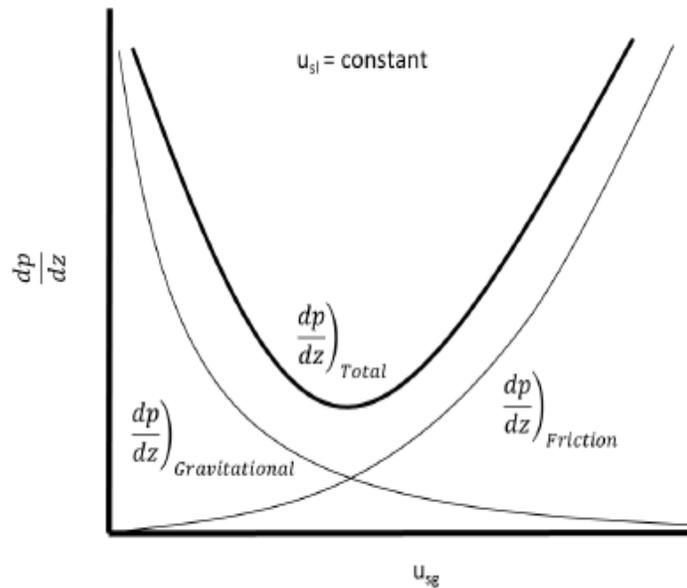
Figure 2.8 Pressure gradient behavior in vertical two-phase flow (Shoham, 2005)

Studies of pressure drop measurement identified that variation of gas and liquid superficial velocities have a significant effect on pressure gradient (Perez, 2008; Ali, 2009; Zangana et al., 2011; and Waltrich et al., 2015). In relation to pipe diameter effect, pipe diameter has a

significant impact on pressure drop (Zangana et al., 2010; and Waltrich et al., 2015). Furthermore, Waltrich et al. (2015) argued that effect of pipe diameter on pressure gradient is negligible for pipe diameter greater than 0.1 m. This is because the interfacial friction loss between gas and liquid phase is significant in large diameter pipes above 0.1 m when compared with friction against the wall of these pipes.

Another important parameter in the study of two-phase gas-liquid flow in vertical pipe is liquid holdup or void fraction. Both the terms are interchangeably used in the studies of two-phase flow depending on the need. Holdup or void fraction is essential as it plays a fundamental role in categorizing the distribution of the phases within the system. If holdup is known, the void fraction can be determined by subtracting it from 1 or vice versa. Liquid holdup varies from 0 to 1. The numeric 0 denotes the single-phase gas in pipe, and the numeric 1 means the single-phase liquid. Several studies in the literature have proposed correlations for predicting void fraction (Sun et al., 1981; Kokal and Stanislav, 1989; Gomez et al., 2000; and Woldesemayat and Ghajar, 2006) for liquid holdup to be estimated. Holdup and void fraction can be measured using different techniques. These include quick-closing valve technique (Waltrich et al., 2015), gamma ray absorption technique (Hewitt and Whalley, 1980; and Chan and Banerjee, 1981), impedance method and differential pressure measurement (Ali, 2009). Generally, liquid holdup decreased significantly with superficial gas velocity (Perez, 2008; and Waltrich et al., 2015). Related to pipe diameter, liquid holdup increases slightly for large variations of liquid superficial velocities for the same pipe diameter. However, there is no substantial change in liquid holdup for pipe diameter greater than 0.1 m (Waltrich et al., 2015). Digitized liquid holdup plot for Perez (2008) and Waltrich et al. (2015) are shown in **Figures 2.9a** and **b** respectively. Studies on void fraction showed that at a fixed liquid velocity, void fraction increases as superficial gas velocity increases. However, it decreases with increasing superficial liquid velocity at fixed gas velocity (Zubir and Zainon, 2011; and Damir, 2012).

(a)   (b)
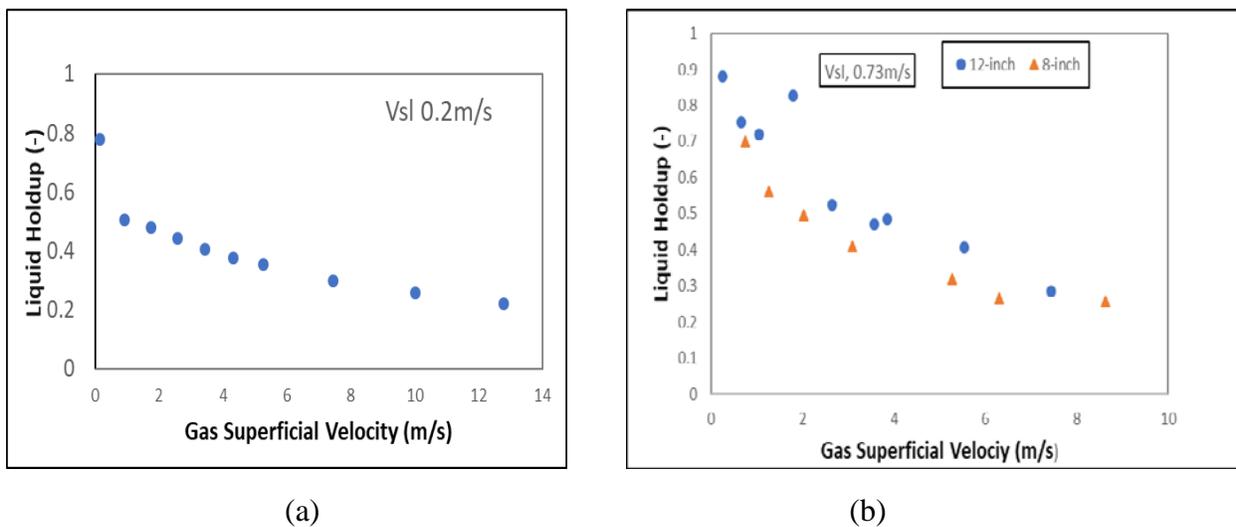
Figure 2.9 Liquid holdup vs. gas velocity (a) Perez, 2008 and (b) Waltrich et al., 2015

During this investigation, many multiphase flow studies conducted in vertical pipe have been reviewed. The summaries of the review for vertical pipe with small (< 0.15 m) and large (> 0.15 m) diameters are shown in Tables 2.3 and 2.4, respectively. Some studies (Omebere-Iyari et al., 2007; Ali, 2009; and Zabaras et al., 2013) emphasized that multiphase flow in small diameter pipes could be different in comparison with large diameter pipes. Therefore, extrapolating small diameter results to predict large pipe flow behavior could be misleading. It can be observed from the tables that almost all the studies were performed in the domain of low gas and liquid velocities with Mach number less than 0.3. Studies of multiphase flow under the condition of high gas and liquid velocities with Mach 1 are scarce. Multiphase flow data obtained from the studies under the condition of low gas and liquid velocities cannot be used to predict worst case discharge. Due to this reason, experimental works need to be done in the domain of high gas and liquid velocities with Mach number above 0.3. Therefore, WCD can be predicted accurately. State of the art experimental techniques is needed to study the flow structure and domains involving Mach numbers greater than 0.3 and equal to 1 (subsonic and supersonic flow). Subsonic flow is a flow condition pipes with Mach number between 0.3 to 1 while supersonic flow condition occurs at Mach number greater than 1.

Table 2.3 Summary of the literature survey for diameter pipe (< 0.15 m)

Researcher	Year	Fluid System	Pipe Diameter (m)	Vsl (m/s)	Vsg (m/s)	Pressure (MPa)	Flow Regime Observed	Remarks
Fukano and Kariyasaki	1992	Air-water	0.001,0.0024 and 0.0049	-	-	0.1	Bubbly and Slug	1. No small bubbles in liquid slugs and liquid films 2. Liquid slug is easier to form in small diameter pipes than large diameter 3. No separated flow observed
Mishima and Hibiki	1996	Air-water	0.001 and 0.004	-	-	0.1	Bubbly and Slug	1. Flow patterns common to capillary tubes were observed 2. The two-phase frictional pressure loss measured in the experiment was in good agreement with Chisholm's correlation with a new development of equation for C parameter as function of the tube diameter
Sun et al.	2002	Air-water	0.1125	0.011 and 0.15	0.122	0.1	Bubbly, Distorted cap bubbly and Churn	1. Slug formation is due to increase of void fraction waves by coalescence of bubbles clusters from unstable bubbly flow 2. Taylor bubbles formation can be hindered due to intense turbulence.
Lucas et al	1995	Air-water	0.0512	Wide range	Wide range	2.5	Bubbly, Cap bubbles and Slug	1. Small bubbles were found near the wall of the pipe while larger bubbles were concentrated in the core of the pipe.
Perez	2008	Air-water	0.038 and 0.068	0.15 - 8.9 m/s	0.04 - 0.7 m/s	0.1	Bubbly, churn, slug and highly aerated slugs or waves	1. Liquid holdup decreased significantly with superficial gas velocity, regardless of pipe diameter and liquid velocity
Szlinski et al	2010	Air-water and Air-silicone	0.067	0.2-0.7	0.05-5.7	0.1	Bubbly, Cap bubbles, Slug, Churn and Annular	1. Bubbles formed with air-water are larger than in air-silicone oil at the same liquid superficial velocities and it is due to different in liquid viscosities 2. some of the flow pattern prediction models do not give reasonable predictions of transition of slug to churn and churn to annular

Table 2.3 Continued.

Zangana et al.	2011	Air-water	0.13	0.01-0.7	3-16.25	0.1	-	1. Frictional pressure drop is significantly affected by variation of gas and liquid superficial velocity. 2. Pipe diameter has significant effect on total pressure drop. 3. Normally, total pressure drop decline as the pipe diameter increases for given liquid and gas superficial velocities. Nevertheless, due to differing balance between gravitational and frictional components of the pressure drop there are some exceptions to this theory
Zubir and Zainon	2011	Air-water	0.021, 0.047 and 0.095	0.006 to 1	0.1 to 2	0.1	Bubbly and Churn	1. Void fraction consistently increased with superficial gas velocity and decreased with superficial liquid velocity. 2. Slug length was influenced by pipe diameter
Damir	2012	Air-water	0.13	0.017 – 0.51	3-16	0.01 and 0.02	Annular and Churn	1. Void fraction increased with superficial gas velocity and decreased with superficial liquid velocity
Waltrich	2015	Air-water	0.051 and 0.1	0.13-1.61	0.063- 25	0.1	Bubbly, Slug, Churn and Annular	1. Pipe diameter has more effect on pressure gradient in small pipes ($\leq$ 0.1m ID) than big pipes 2. Liquid holdup for 0.1 m ID pipe has different trends from that of the larger diameters (0.2 and 0.3m ID) studied. The different in trends is due to the presence of slug that occurs between the bubbly to-non-bubbly and churn-to-annular transition zones
Ansari and Azadi	2016	Air-water	0.04m and 0.07m	0.015 - 1.530	0.038–20.44	0.1	Bubbly, Churn and Slug	1. Increase in axial location does not affect transition boundaries.

Table 2.4 Summary of the literature survey for diameter pipe (> 0.15 m)

Researcher	Year	Fluid System	Pipe Diameter (m)	Vsl (m/s)	Vsg (m/s)	Pressure (MPa)	Flow Regime Observed	Remark
Shipley	1983	Air-water	0.457	2	5	0.1	Bubbly	1. Decrease in rise velocity caused bubble concentration to increase.
Ohnuki and Akimoto	1996	Air-water	0.480	0.01 - 0.2	0.02-0.87	0.1	Uniform bubbly, Agitated bubbly, some Cap bubbles and Churn	1. Air injection methods effects are minimal in respect of the shapes of the phase distribution and differential pressure at the upper half of the test section. 2. Axial distribution of the differential pressure and radial distribution of local void fraction showed unusual distribution at lower half of the test section which depend on air injection methods
Cheng et al	1998	Air-water	0.0289 and 0.15	1.25	1.113	0.1	Bubbly, Cap bubbles, and Churn	1. It was observed that slug flow does not occur on 0.15m diameter column. However, the flow gradually transit to churn as the gas velocity increased. 2. Bubble to slug was identified with associated void fraction wave instabilities in 0.0289m diameter column at constant liquid rate.
Shen et al.	2006	Air-water	0.2	0.144 to 1.12	0.0322-0.218	-	Undisturbed bubbly, Agitated bubbly, Churn bubbly, Churn slug and Churn froth	1. Two phase void phase distribution characteristics could be identified as either core peaked or wall peaked
Shen et al.	2010	Air-water	0.199	0.0501 - 0.311	0.0016-0.093	0.1	Bubbly, Churn and Slug	1. Flow regimes flow depended on the gas and liquid superficial velocities

Table 2.4 Continued.

Zabaras et al.	2013	Air-water	0.2794	-	-	0.1	Churn	1. Flow regimes in small diameter pipes (< 0.1 m) are differ from large pipes. 2. Experimental holdup is larger than predicted hold up by OLGA and other in-house models.
Waltrich et al.	2015	Air-water	0.2 and 0.3	0.13-1.61	0.063- 25	0.1	Bubbly, Churn and Annular	1. Pipe diameter has more effect on pressure gradient in small pipes (≤ 0.1m ID) than big pipes. 2. Liquid holdup for 0.1 m ID pipe has different trends from that of the larger diameters (0.2 and 0.3m ID) studied. The different in trends is due to the presence of slug that occurs between the bubbly to-non-bubbly and churn-to-annular transition zones.

2.7. Two-Phase Flow in Annulus

Majority of the studies in the literature on multiphase flow are done in vertical pipes. However, studies on multi-phase flow in vertical annuli are scarce and the few experimental works been done on annulus are only for low liquid and gas velocities with low Mach number (Ma < 0.3) flows. The flow patterns in vertical annulus are similar to those observed in vertical pipe (Caetano, 1985; Ozar et al., 2008; and Julie et al., 2010). However, the slug and annular flow patterns are different in comparison with vertical pipes (Caetano, 1985). The slug flow in annulus exhibits a distorted Taylor bubble with rising velocity faster than that observed in pipe flow. Annular flow in annulus pipe consists of two liquid films which wet the configuration boundary walls. Furthermore, Caetano (1992a) reported that an inner pipe in the annulus responsible for the change of slug and annular flow patterns. Caetano (1985) modified Taitel and Dukler (1980) flow pattern map to allow prediction of flow regime in annulus pipes. The modified flow pattern was developed using air-water and air-kerosene (Superficial liquid and gas velocities). The liquid holdup and pressure gradient measurements for various flow patterns were reported as a function of gas and liquid superficial velocities in the second part of the study (Caetano et al., 1992b). Ozar et al. (2008) investigated the values of distribution parameters (C0 and C1) for flow patterns in the annulus. It was found to be consistent with those of a circular channel. The summary of the literature review for annulus flow is shown in **Table 2.5.**

Table 2.5 Summary of the literature survey for annulus pipe

Researcher	Year	Fluid System	Annular Pipe ID (m)	Annular Pipe OD (m)	Vsl (m/s)	Vsg (m/s)	Pressure (MPa)	Flow Regime Observed	Remarks
Caetano	1985	Air-water andAir-Kerosene	0.042	0.076	0.003 - 2	0.02 -20	0.85	Bubble, Slug, Churn and Annular	1. The flow patterns in vertical annulus are similar to those observed in vertical pipe. However, the slug and annular flow patterns are different in comparison with vertical pipes.
Ozar et al.	2008	Air-water	0.019	0.038	0.26 -3.31	0.05-3.89	0.1	Bubbly and Cap slug, Churn-turbulent	1. The values of distribution parameters (C0 and C1) for flow patterns in the annulus found to be consistent with those of a circular channel
Julia et al.	2010	Air-water	0.019	0.038	0.2-3.4	0.01-0.2	0.1	Bubbly and Cap slug, Churn-turbulent, and Annular	1. Good agreement between experimental data and some selected models for predicting bubbly flow to cap-slug flow

3. Experimental Setup

3.1. Description of the Flow Loop

The schematic of experimental flow loop used in this study is shown in **Figure 3.1**. The setup consists of: i) insulated stainless steel pipe (PTS) and annular (ATS) test sections with approximate length of 6.7 meters; ii) water circulation pumps (P01 and P02); iii) three air compressors (C01, C02 and C03); iv) Coriolis flow meters (F1, F2 and F3); v) high speed video camera (CAM); vi) pressure and temperature sensors; and vii) quick closing and modulating control valves. Dimensions of the test section are shown in **Figure 3.2**. The test sections have internal diameter of 83 mm. A pipe of 35 mm outer diameter is installed in the annulus. The concentricity of the pipe is maintained by 3 mm screws lateral mounted on the pipe at the entrance and exit sections. The test sections are mounted on a structural frame and vertically attached to the wall (**Figure 3.3**).
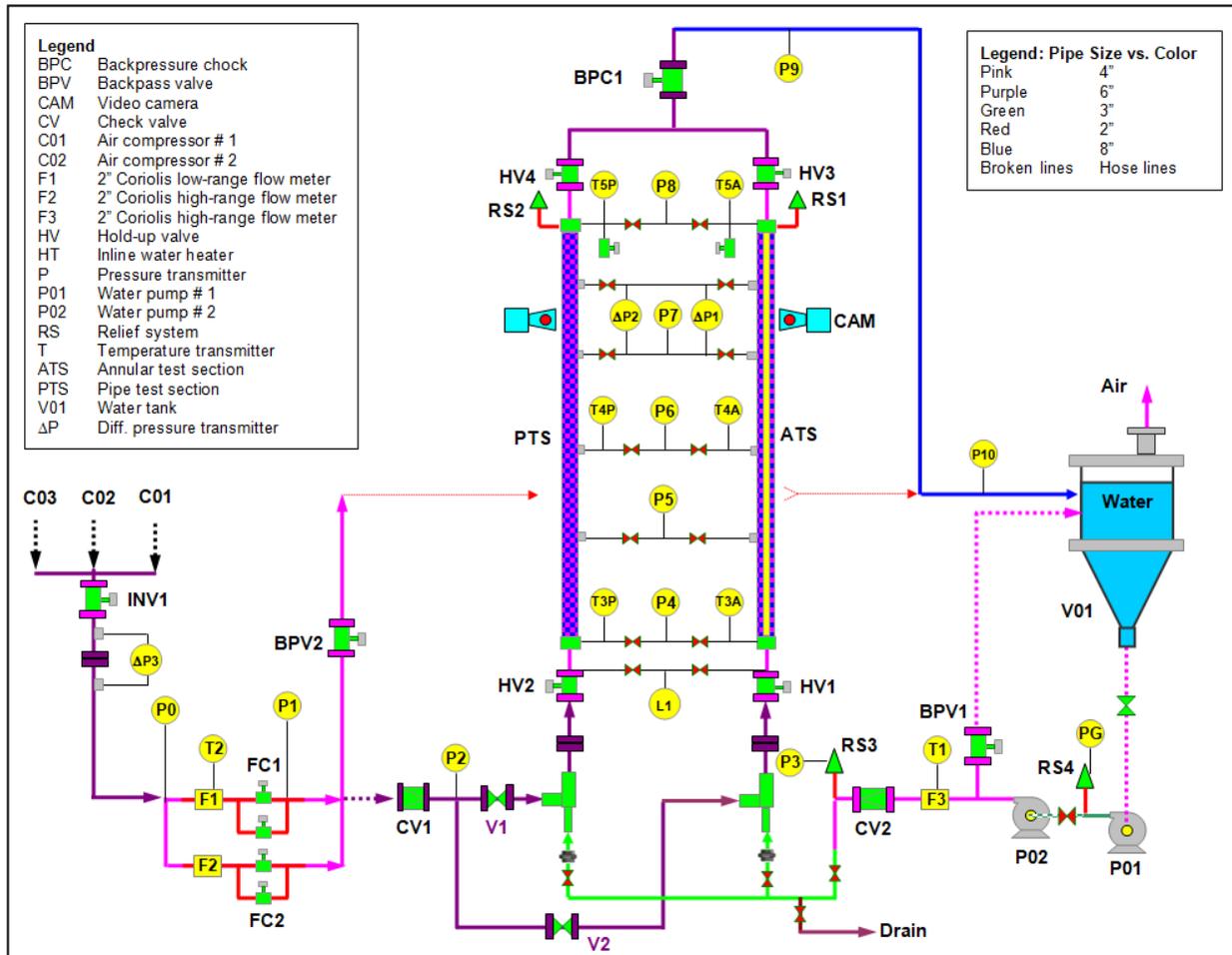
Figure 3.1 Schematic of the experimental flow loop

Measuring instruments installed on the test sections are differential pressure transmitters, gauge pressure transducers and temperature transmitters. The instruments are used to monitor pressure and temperature change occurring in the test sections during experiment. The experimental setup allows the determination of liquid holdup base on liquid level measurement.   Moreover, transparent polycarbonate viewing ports on the test sections permit flow regimes detection by recording video clips during the experiments.   **Table 3.1** summarizes the instrumentation, manufacturer and model, measuring range, and accuracy.

(a)   (b)
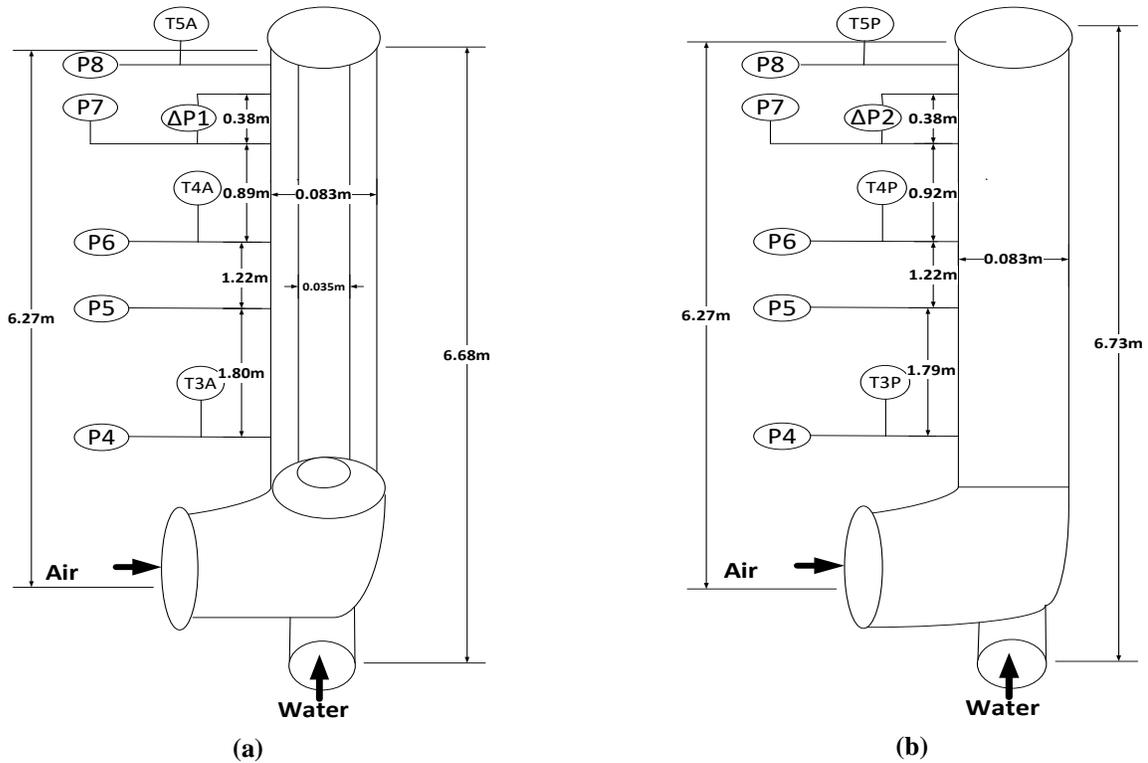
Figure 3.2 Schematic of the test sections: (a) Annulus and (b) Pipe

Table 3.1 List of instruments and experimental measurement uncertainties

Instrument	Name	Manufacturer and model	Accuracy	Range
Air and water Flowmeter 1and 2	F2, F3	Endress Hauser, Promass83F (Coriolis)	±0.35%	0 to 2564 lbm/min
Water Flowmeter 1	F1	Endress Hauser, Promass83F (Coriolis)	±0.35%	0 to 550 lbm/min
Differential Pressure Transmitter	ΔP1, ΔP2, ΔP3	Endress Hauser, Deltabar S, PMD 75	±0.05%	0.025-4 kPa
Gauge Pressure Transducer	P4, P5, P6, P7, P8	SSI Technology Inc , Sensor 200PSIG 1/8NPT	±0.5%	0 to1378.21 kPa
Temperature Transmitter	T4P, T4A	Omega M12TX	±0.2%	−50℃ to 500℃
Temperature Transmitter	T3P, T3A,, T5P, T5A	Omega PRTXD-4 (Fixed)	±0.1%	−50℃ to 200℃
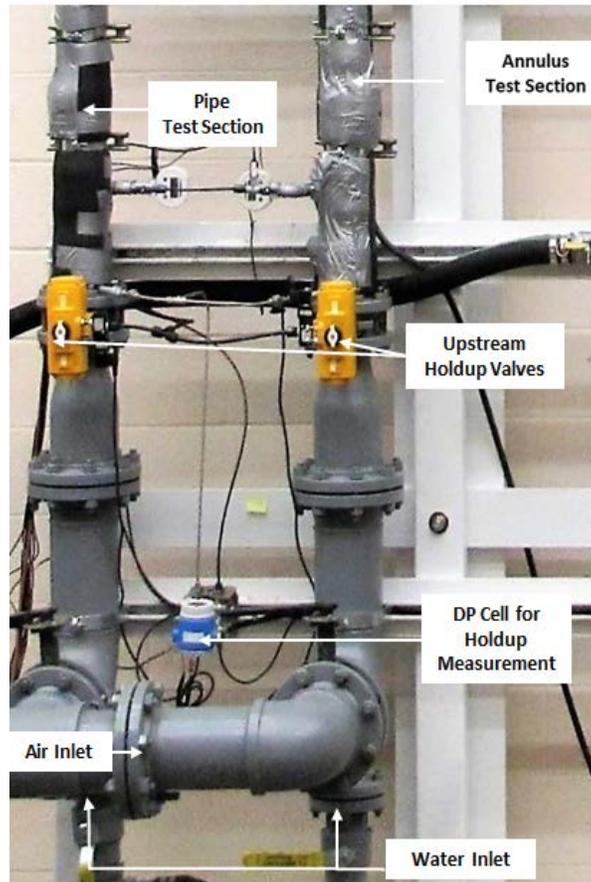
Figure 3.3 Snapshot of the bottom test section

3.2. Flow Loop Components

3.2.1. Air Supply System

Air from compressors C01, C02 and C03 is supplied into the test sections via 150 mm steel pipe. Each of the compressors deliver standard air of 0.76 cubic meters per second with nominal working pressure of 1.03 MPa. The air mass flow rate and gauge pressure are measured upstream of the test sections using two Coriolis flowmeters (F1) and (F2), and pressure gauge, respectively. The flowmeters are installed in parallel to reduce pressure loss. Bypass valve (BPV2) on the air flowline automatically return air to the water tank. The check valve (CV1) prevents water from entering the air supply line.

3.2.2. Water Supply System

Water is supplied to test sections from a 11.35 m^3 storage water tank (V01) which is opened to the atmosphere with the base on the floor. The tank is connect to the primary pumped (P01, Black Hawk Model 306545011000R), which feeds the secondary (P02, Gould 3656 S). Both pumps (**Figure 3.4**) are centrifugal type with Variable Frequency Drives (VFD) to control flow

rate accurately. The pumps are capable of delivering flow rate of up to 0.6 m^3/min at 1 MPa. The water flowline consists of a ball valve that connects water tank to P01 via 100 mm diameter hose. P01 is linked to P02 via 89 mm steel pipe. Coriolis flow meters (F3) on the water flowline measure the flow rate of liquid. Bypass valve (BPV1) returns water to the water tank when activated. The check valve (CV2) prevents air from entering into the water flow line.

<div align="center">(a)   (b)</div>

Figure 3.4 Centrifugal pumps: (a) Primary; and (b) Secondary

3.2.3. Gas-Liquid Mixing Section

Water is injected into the test sections through 89 mm diameter steel pipe and the air via 150 mm steel pipe. The air and water are thoroughly mixed before been entering into the test sections. This allows the two-phase flow to reach steady state condition before getting to the points of measurement. Perforated stainless steel plates of different mesh sizes and diameters are installed at the entrance of the liquid phase. This allows the liquid to be sprayed into the test sections and carried by the gas phase, which is traveling at high speed.

3.2.4. Data Acquisition

Measurements from all the instrumentation such as differential pressure transducers, gauge pressure transducers, temperature transmitters, and flowmeters installed on the flow loop are processed and recorded with a data acquisition PC equipped with a multi-channel Data Acquisition (DAQ) card. The real-time analog data are converted to digital numeric values, gathered and displayed on computer monitor with the aid of a VBA program.

3.2.5. Water Tank

The water tank is shown in **Figure 3.5** is used to store and circulate test liquid. The tank is exposed to the atmosphere with the base on the floor. It has volume capacity of 11.35 m^3 (3000

gallons). The tank is connected to the primary centrifugal pump via 100 mm diameter hose pipe that has a ball valve. The valve must be opened before switching on the centrifugal pump, so as to prevent the primary pump from damage.

Figure 3.5 Water tank

3.2.6. Flowmeters

There are three Coriolis flowmeters (Endress Hauser Promass 83F) installed in the experimental flow loop to measure gas and liquid flowrates (**Figure 3.6**), two for measuring gas flow rate and one for the liquid rate. The liquid flow meter and one of the gas flow meters have measuring range of 0 to 1,160 kg/min with an accuracy of ±0.15%. The other flow meter has measuring range of 0 to 248 kg/min with an accuracy of ±0.15%.

Figure 3.6 Coriolis flowmeter

3.2.5. Pressure Sensors

Three differential pressure transmitters (DP) manufactured by Endress Hauser (Deltabar S, PMD 75) are installed on the flow loop (ΔP1, ΔP2, and L1). The DP sensors (**Figure 3.7a**) are installed in the test section. The L1 is located at the base of the test section, and it measures liquid holdup. DP2 and L1 have an accuracy of 0.05%

and ranged from -5 to 5 kPa. DP1 measures from -1 to 1 kPa. Gauge pressure transducers (P4, P5, P6, P7 and P8, shown in **Figure 3.8b**) have measuring range of 0 to 0.68 MPa with an accuracy of ±0.5%. They operate from -40 to 105°C.

(a)   (b)
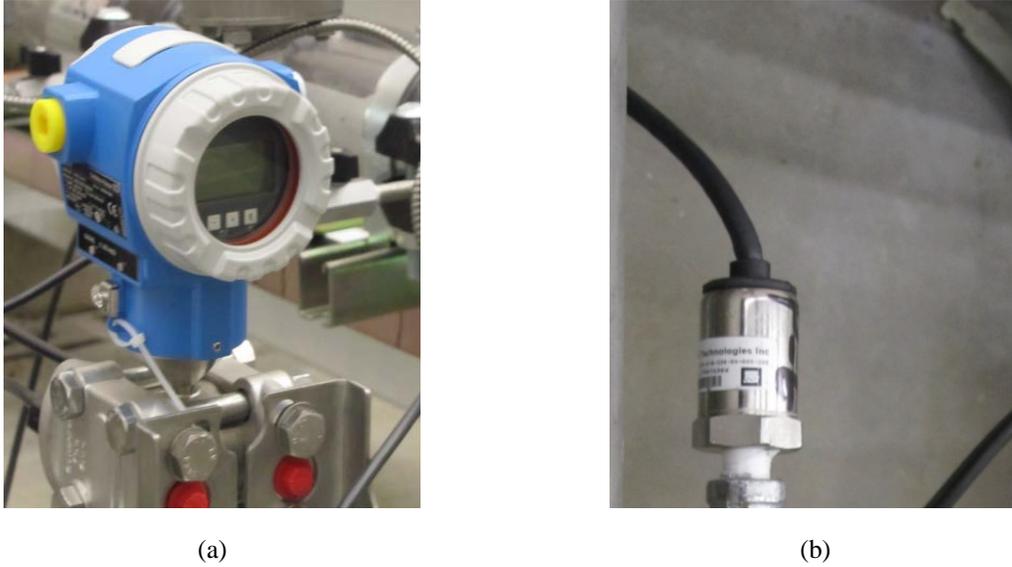
Figure 3.7 Pressure sensors (a) differential pressure transmitter (b) pressure transducer

3.2.6. Temperature Sensors

Four PRTXD-4 (**Figure 3.8a**) and two M12 TXC series RTD (**Figure 3.8b**) temperature transmitters manufactured by Omega are installed on the annulus and pipe test sections. The PRTXD-4 and M12TXC transmitters measure from -50 to 200°C with accuracy ±0.1% and -50 to 120°C with accuracy ± 0.2%, respectively.

(a)   (b)
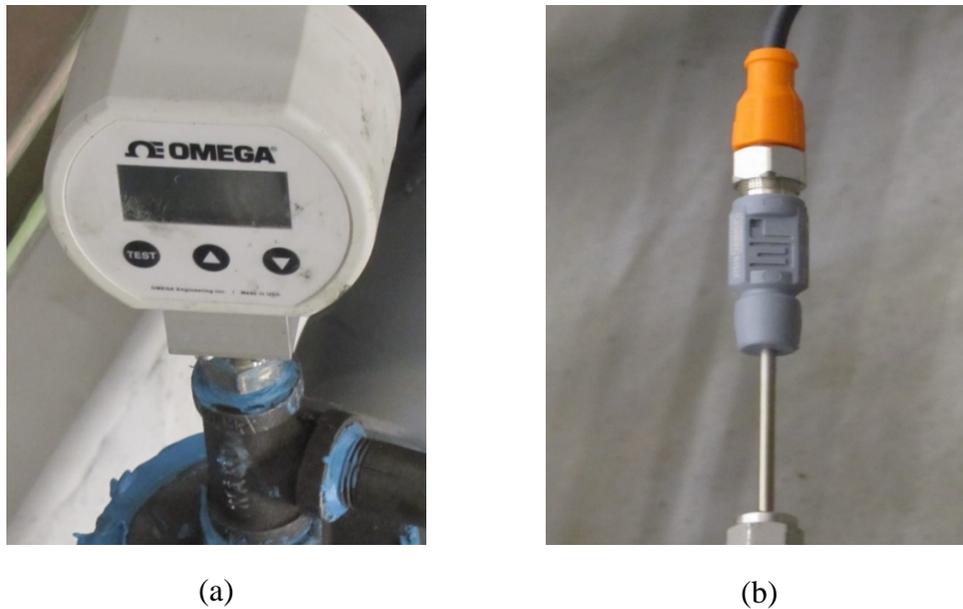
Figure 3.8 Temperature transmitters: (a) Omega PRTXD-4; and (b) Omega M12TXC

3.2.7. Holdup Valves

There are four fast reacting butterfly valves (HV1, HV2, HV3 and HV4) installed on upstream and downstream of the test sections (**Figure 3.9**). The valves operate at a temperature range of -50 to 200°C and pressure range of 1.6 MPa. Two of the valves are operated simultaneously to measure the liquid holdup in the test sections during the experiment.

3.2.8. Bypass Valves

BPV1 and BPV2 are butterfly valves installed to direct the liquid and gas phase to the water tank when the fluid in the test section is trapped by the abrupt closing of the holdup valves. They are installed to minimize hammering effects of the pumps and compressors.

Figure 3.9 Quick closing valve

However, they were not used during the experiment because of severe hammer they generate in the water tank and return line when they divert the two-phase flow. Instead of these valves, another quick closing valve is installed on the gas inlet line to shut off the gas supply during the holdup. Also, instead of the water bypass valve, the water pumps were stopped during the holdup automatically using the Variable frequency drives (VFD).

3.2.9. Relief Valves

Two relief valves (**Figure 3.10**) were installed at the exits of the test sections. The relief valves are set to open at 10 bar. This is to prevent over-pressurization and damage of the test sections and other flow loop components.

3.2.10. Air Compressor

Three air compressors (CO1, CO2, and CO3) with standard air capacity of 0.76 cubic meters per second each at 1.03 MPa were utilized during the experiment. The snapshot of the compressors employed to supply air during the experiment is depicted in **Figure 3.11**.

Figure 3.10 Relief valve

Figure 3.11 Air Compressors

3.3. Experimental Procedure

Prior to the start of the experiment, the flow was diverted to the desired test section by opening one of the inlet valves. The test section was emptied by draining liquid from the loop. Then, air control valves were slowly opened to initiate air flow. Water pumps were started once air flow was initiated. Air and water flow rates were automatically adjusted to the desired rates using the data acquisition system. The test condition was maintained until water and air flow rates become reasonably stable and steady-state condition was established. At the steady state condition, test parameters were logged; videos of the fluid flowing in the test section were captured and recorded, and the holdup valves were closed quickly to trap the fluid in the test section. As the same time, the inlet valve was closed quickly while the liquid pumps were stopped abruptly. The liquid level in the test section was measured using differential pressure transducer (L1). Then, the backpressure valve was closed to expand the trapped fluid by opening the holdup valves. After the expansion, the backpressure valve was slowly opened to release the trapped fluid.

3.4. Experimental Program Description

Preliminary experimental tests were conducted to verify the accuracy of measurements. Water was used as test fluid in the preliminary test. The data obtained from the preliminary tests are analyzed and compared with predictions of established correlations for smooth pipe and annulus. After completion of the preliminary test, the main experiments were performed. The experimental test matrix is shown in **Table 3.2**.

Table 3.2 Experimental test matrix

Test	Superficial Water Velocity (m/s)	Superficial Air Velocity (m/s)	Type of test
Preliminary Test	0.47-1.2	-	Single (Water)
Low Velocities	0.23 – 2.0	8 - 20	Multiphase flow
Medium Velocities	0.23 – 2.0	21 - 80	Multiphase flow
High Velocities	0.23 – 2.0	80 - 160	Multiphase flow

4. Preliminary Test

4.1 Single Phase Experiments

The single-phase experiments were carried out by circulating water at ambient temperature varying flow rate (40 - 100 gpm). During the test, pressure drop measurements were obtained from three differential pressure transducers (ΔP_1, ΔP_2, and L_1). The distance between pressure ports for ΔP_1 and ΔP_2 are 0.38 m. As a result, pressure drop measurements were very small and inaccurate. The distance between pressure ports of L1 is 5 m and the measurements (**Figure 4.1**) were significant. The results demonstrate an anticipated pressure drop behavior of flow in pipe and annulus under turbulent flow conditions. To validate the accuracy of the measurements, measured pressure losses are compared with the ones calculated from Equation (4.1). The comparison shows reasonable match with some discrepancies. Measurements are higher (10 to 30%) than prediction due to entrance effects, pipe roughness and other irregularities, which tend to increase pressure losses.

(a)   (b)
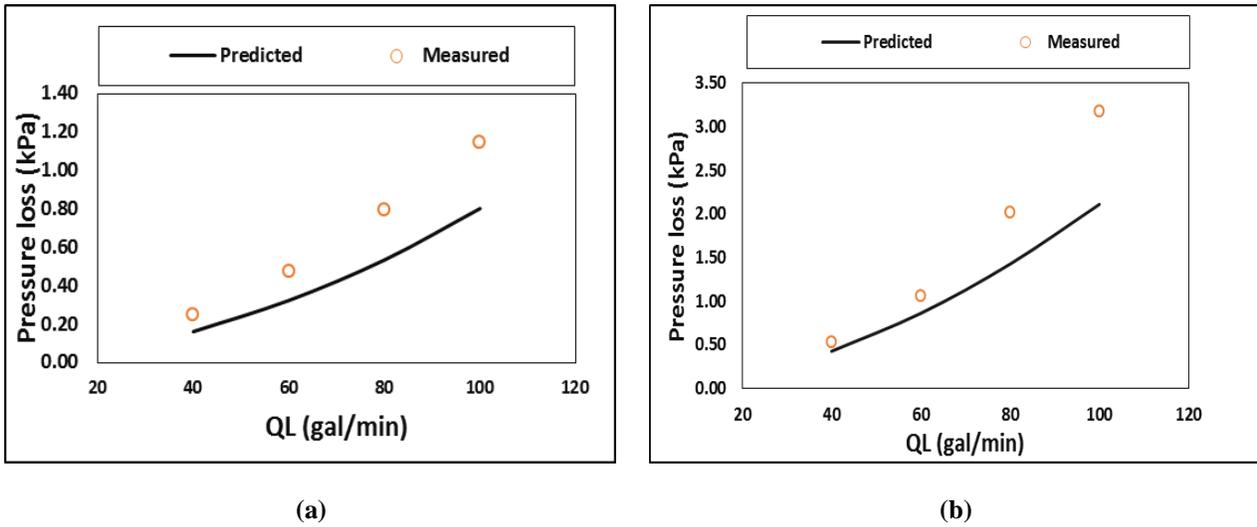
Figure 4.1 Measured and calculated pressure drops: (a) pipe and (b) annulus

Pressure loss (ΔP) in any circular duct is related to diameter (D), length (L), fluid density (ρ) and mean fluid velocity (V). Thus:

$$\Delta P = f \frac{2L}{D} \rho V^2 \tag{4.1}$$

where f is the fanning friction factor. In this analysis, L is the distance between pressure transducer ports. The friction factor used in the calculation of pressure loss is expressed as (Chen, 1979):

$$\frac{1}{\sqrt{f_D}} = -2.0 \, log \left[\frac{\varepsilon}{3.7065D} - log \left(\frac{1}{2.8257} \left(\frac{\varepsilon}{D}\right)^{1.1098} + \frac{5.8506}{R_e^{0.8981}} \right) \right] \tag{4.2}$$

41

where f_D is the Darcy friction factor, which is defined as fourfold of the Fanning friction factor. ε is the pipe roughness, R_e is the Reynold number. **Table 4.1** depicts the comparison between the measured and predicted pressure losses.

Table 4.1 Measured and predicted pressure loss in pipe and annulus flow

Q_L (GPM)	Type	V_L (m/s)	R_e	Measured ΔP (Pa)	Predicted ΔP (Pa)	Error (%)
40	Pipe	0.47	39010	248.84	161.51	35.09
60	Pipe	0.7	58100	472.80	324.24	31.42
80	Pipe	0.93	77190	796.29	534.76	32.84
100	Pipe	1.17	97110	1144.66	802.74	29.87
40	Annulus	0.56	27440	530.01	426.17	19.59
60	Annulus	0.84	41160	1060.02	861.93	18.69
80	Annulus	1.12	54880	2014.05	1425.77	29.21
100	Annulus	1.4	68600	3180.07	2110.74	33.63

4.2 Liquid Holdup Validation

The volumetric liquid holdup value is considered one of the critical and important parameters of two-phase flow. It affects pressure drop significantly. Thus, an accurate liquid holdup measurement is very necessary in multiphase flow studies. Generally, there are different methods to measure liquid holdup. The simplest method is the volumetric method by collecting the residual amount of water trapped in the test section after each experiment. Although this method is the most accurate approach, it is still not robust. Another approach is differential pressure (DP) based method. In this method, A DP cell sensor is utilized to measure residual liquid column in the test section using hydrostatic pressure concept. In this study, a differential pressure sensor (L_1 aka ΔP_3) at the bottom of the test section (**Figure 4.2**) was used to measure liquid holdup. To ensure the accuracy of liquid holdup measurement using DP sensor, holdup measurement obtained from ΔP_3 was compared with actual volumetric liquid holdup, which was obtained by draining the liquid collected in the test section. Two-phase flow experiment was carried out validate liquid holdup measurement. The amount of liquid trapped in the test section after the closing of the valves was calculated using bottom-hole pressure acquired by the pressure sensor ΔP_3 on the bottom of the pipe. Thus, the volumetric liquid hold is:
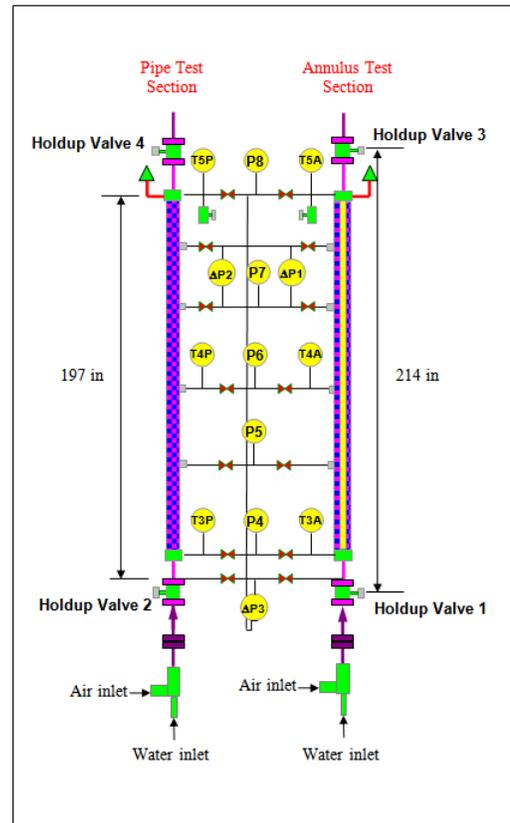
Figure 4.2 Schematic of test section (pipe and annulus)

42

$$H_L = \frac{V_L}{V_T} \tag{4.3}$$

where H_L is the liquid holdup, V_L is the liquid volume, V_T is the total volume of the test section. Pressure-based liquid holdup is expressed as:

$$H_L = \frac{\left(P_{wf}/\rho_l g\right)A}{(H_T A)} = \frac{P_{wf}}{\rho_l g H_T} \tag{4.4}$$

where P_{wf} is the bottom-hole pressure, A is the cross-section area of the test section, ρ_l represents liquid density, g is the gravitational acceleration, and H_T is the total height of the test section. After the liquid holdup measurement was obtained from the DP sensor, the residual liquid was drained and measured. By known the total volume of the test section and residual amount of the liquid in the test section, the volumetric liquid holdup was calculated using Equation (4.3). Afterward, it was compared to the average liquid holdup obtained from ΔP_3 in terms of percentage. **Table 4.2** shows the comparison between the estimated and measured liquid holdup. It can be observed that the discrepancy between the two methods stays within 1% error.

Table 4.2 Comparison between the estimated and measured liquid holdup

Q_L (GPM)	Q_G (lb/min)	HL (DP Cell) %	(HL) %	Error %
35	25	7	8.0	1.0
40	10	14	12.9	1.1

4.3 Validation of Measurements of Annular Flow Experiments

There are limited experimental data on the annular flow of multiphase fluid. Measurements from one of the published studies (Caetano, 1985) have been used to validate data obtained from the annular test section. For validation, 6 measurements were chosen matching the liquid and gas superficial velocities of the flows. **Table 4.3** presents the selected data set from Caetano's experiment showing pressure loss and liquid holdup measurements. The superficial gas and liquid velocities are shown in Table 4.3 were used to calculate the flow rate of water and air required to match the velocities in the current investigation. Our experimental data (**Table 4.4**) shows lower pressure gradient than the corresponding values for the Caetano's experimental data. However, the liquid holdup values are higher in the current study. This can be attributed to the slight difference in annular geometry. Caetano (1985) used narrow (3" × 1.66") annulus while the current study uses wide (3.25" × 1.37") annulus. The higher annular space might have resulted in the higher holdup in the present study. In addition, to further validate the results, the trends of Caetano's measurements are examined. There are three datasets in his experiments in which the liquid velocities were same while the superficial gas velocities were different (**Table 4.5**). The experimental data suggests that with an increase in gas superficial velocity, the pressure gradient increases. A similar trend is observed in the current study in which the pressure gradient increased with the superficial gas velocity. The increase is due to excessive friction pressure loss, which dominates the gravitational component of the total pressure drop.

43

Table 4.3 Published experimental data (Caetano, 1985)

Cases	Gas Velocity	Liquid Velocity	Liquid Holdup	Pressure gradient	
	m/s	m/s		Pa/m	Psi/ft
1	13.023	0.299	0.13	3176.6	0.140
2	8.093	0.299	0.17	2736.4	0.121
3	16.61	0.523	0.12	4671.7	0.207
4	16.68	0.548	0.13	5115.8	0.226
5	13.535	0.967	0.17	7082.9	0.313
6	12.708	1.17	0.19	7499.3	0.332

Table 4.4 Measurements from the current study

Cases	Gas Velocity	Liquid Velocity	Liquid Holdup	Pressure gradient	
	m/s	m/s		Pa/m	Psi/ft
1	13.05	0.32	0.16	2275	0.101
2	9.41	0.29	0.21	2268	0.100
3	16.83	0.51	0.18	3039	0.134
4	16.61	0.52	0.20	3043	0.135
5	13.86	0.97	0.19	3918	0.173
6	13.02	1.12	0.25	4446	0.197

Table 4.5 Published experimental data (Caetano, 1985)

Cases	Gas Velocity	Liquid Velocity	Liquid Holdup	Pressure gradient	
	m/s	m/s		Pa/m	Psi/ft
1	14.9	0.003	0.03	571	0.025
	9.0	0.003	0.00	516	0.023
2	13.0	0.299	0.13	3177	0.140
	8.1	0.299	0.17	2736	0.121
3	14.4	0.031	0.05	1003	0.044
	8.9	0.031	0.09	952	0.042

5. Two-Phase Flow in Pipe

This section discusses the results of two-phase flow experiments conducted in the pipe section. Experimental measurements are analyzed in terms of three parameters, namely flow regimes, liquid holdup, and pressure gradient.

5.2 Flow Regimes in Pipe

The classification of flow regimes is an important part of two-phase flow analysis. It is necessary to develop or select an appropriate flow model to predict two-phase behavior in vertical pipe and annulus. Two-phase flow regimes depend on parameters such as liquid and gas superficial velocities, duct geometries, and fluid properties. In Section 2.3 different types of flow regimes that can be established in pipe and annulus are discussed.

In this study, flow regimes were identified by visual observation the flow pattern during the experiments and recording of video clips using a high-speed camera. The snapshots of flow regimes observed in the pipe are shown in **Figures 5.1** and **5.2**. The flow patterns observed during the investigation were churn, transition of churn to annular and annular flow regime. At high gas superficial velocity with moderate liquid superficial velocity, a chaotic frothy mixture of gas-liquid moved upward and downward in the entire pipe creating a churn flow pattern. Gas core in the flow was not visibly clear due to chaotic movement of the flow. As the gas velocity increased, a flow regime identical to annular flow occurred intermittently. The fluid in this flow regime was moving faster and more chaotic manner as compared to churn flow regime. Annular flow regime occurred at high gas and liquid velocities. Liquid film was formed around the walls of inner and outer pipes due to high energetic gas-phase velocity. The gas core formed in the middle of the annular space was flowing with entrained droplets. Extremely low gas flowrate (less 8 lbm/min) tests were not performed due to the gas flowmeter measuring range limitation.

(a)   (b)
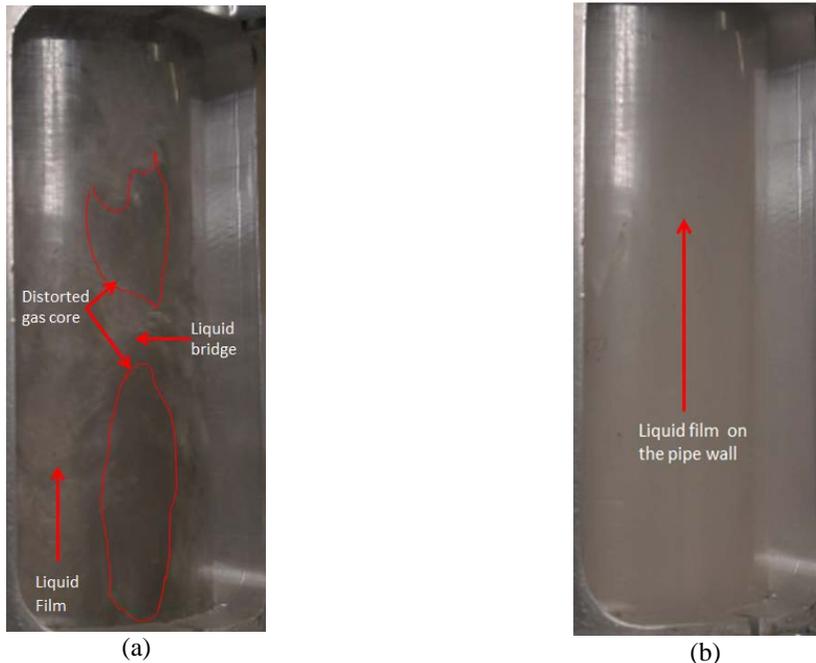
Figure 5.1 Snapshots of flow regimes (a) Churn flow (b) Annular flow
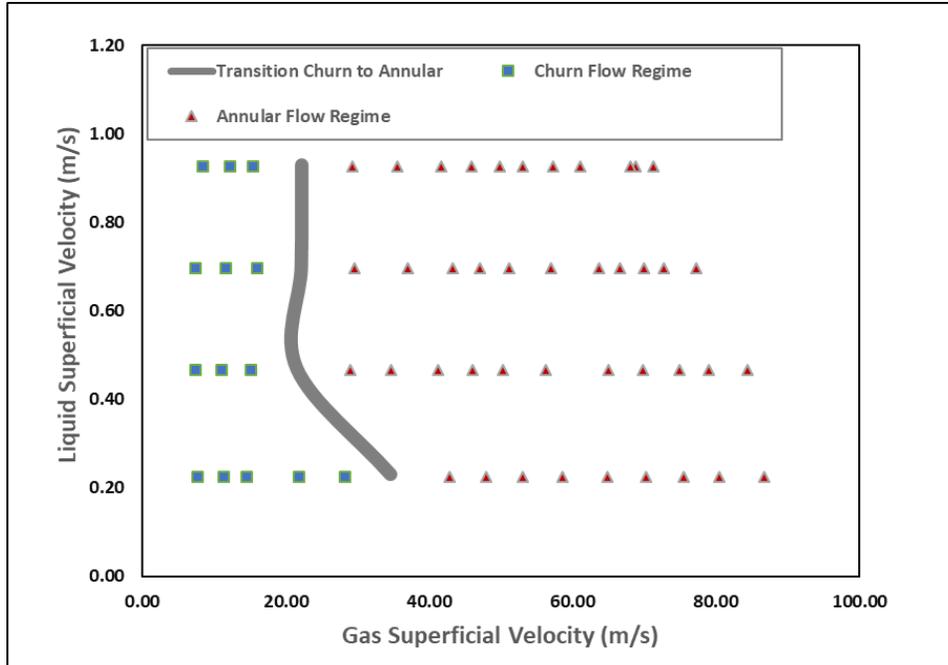
Figure 5.2 Flow regime map of two-phase pipe flows

5.3 Comparison of Flow Regimes

The flow patterns observed in this study are compared with that of published studies (Ali, 2009; Zabaras et al., 2013; LSU, 2015). The flow patterns data points from this study are at higher superficial gas velocity as compared to those of published studies. Furthermore, operating conditions and pipe size are different.
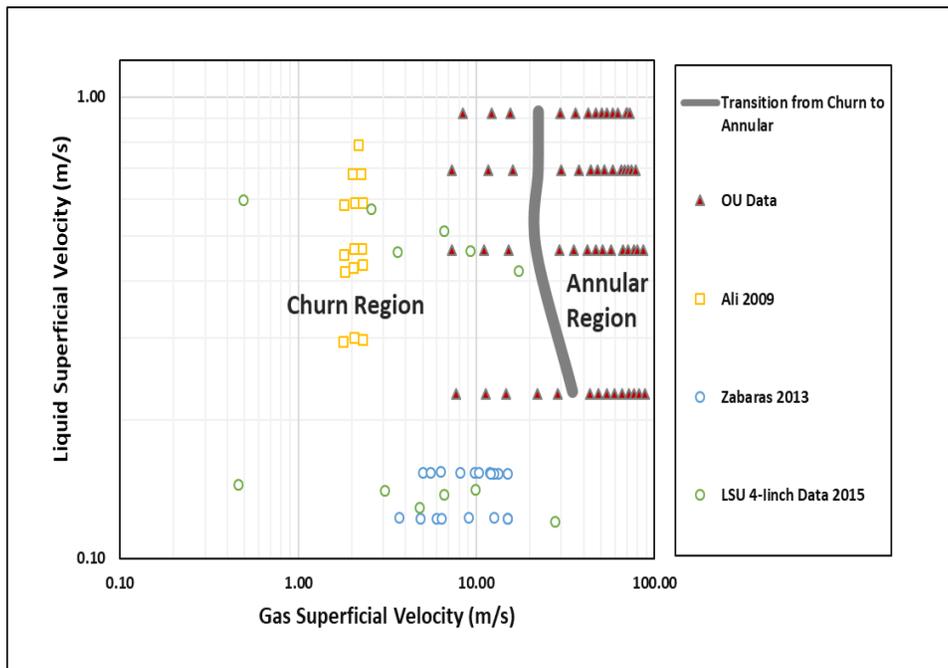
Figure 5.3 Comparison of flow regimes observed in different study

5.4 Liquid Holdup Measurement

The liquid hold-up was measured by using closing valve technique. This technique had been explained in Section 4.2. The liquid holdup measurements for pipe are depicting in **Figure 5.3**. As can be seen from this figure, the liquid holdup decreased asymptotically with superficial gas velocity. There is a slight increase in the liquid holdup with liquid superficial velocity.
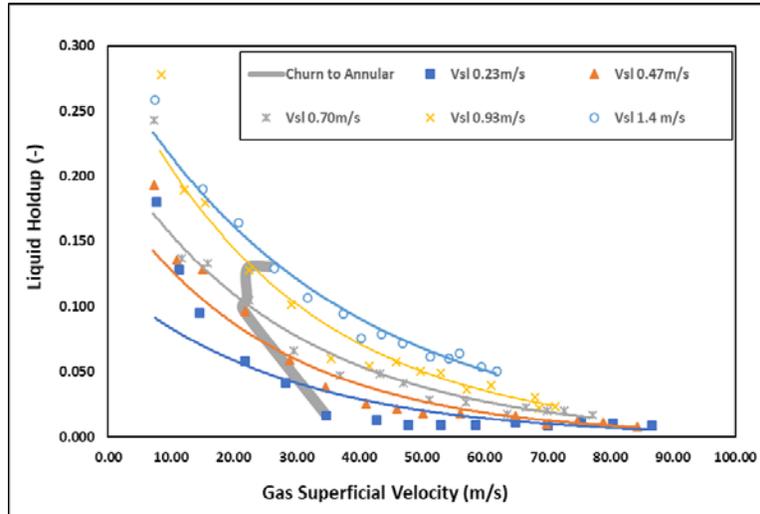
Figure 5.4 Liquid holdup measurements in pipe

5.5 Comparison of Liquid Holdup

The liquid holdup obtained from pipe flow (**Figure 5.5**) is found to be in churn, transition from churn to annular and annular flow regimes. The liquid holdup is compared with the measured liquid holdup from another study (LSU data, BOEM 2015). Reasonable agreement is shown between the trends of two measurements even though superficial velocities were in different ranges.
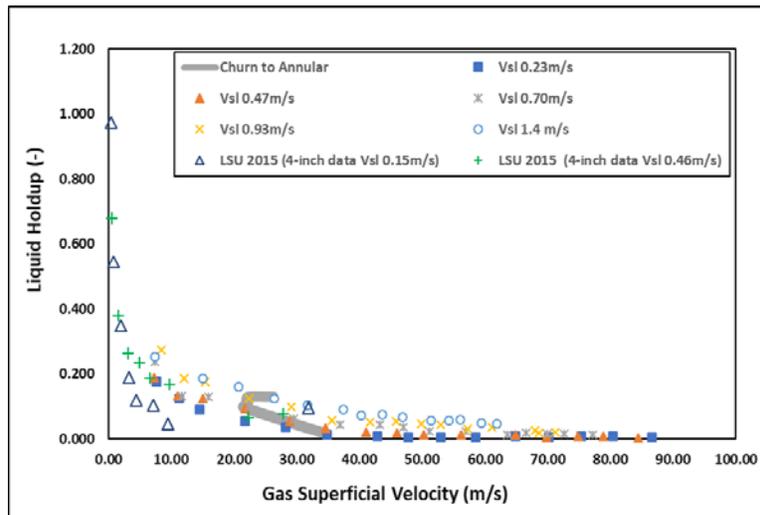
Figure 5.5 Comparison of liquid holdup with LSU data

5.6 Pressure Gradient in Pipe

In this study, the pressure gradient is measured and recorded during the experiments. The experiments were performed in such a way that the superficial liquid velocity was fixed. For each fixed value of superficial liquid velocity, gas superficial velocities were varied from 7 to 160 m/s. The liquid superficial velocities tested are 0.23, 0.47, 0.70, and 0.93 m/s. The analysis of pressure gradient (**Figure 5.6**) shows a predominantly steady increase in pressure gradient with superficial gas velocities. However, a slight reduction in pressure gradient was observed at low superficial gas velocities (less 20 m/s) when low liquid superficial velocity (0.23 m/s). Furthermore, at fixed gas superficial, pressure gradient slightly increase with liquid superficial velocity. The friction component of the total pressure gradient of the two-phase flow dominated the flow at high superficial gas and liquid velocities. Nevertheless, most of the previous studies (Ali, 2009; LSU, 2015) reported a different trend. Gravity component of the total pressure gradient of the two-phase flow dominated the flow in previous studies conducted at low gas and liquid superficial velocities.
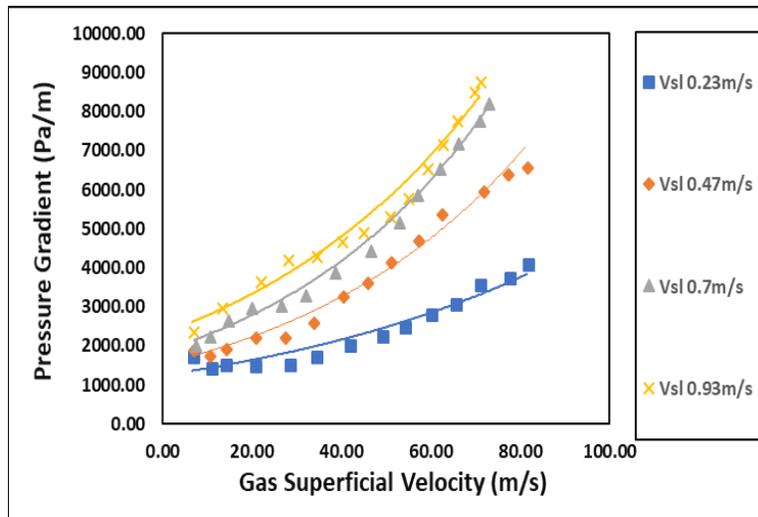
Figure 5.6 Pressure gradient measurements in pipe

5.7 High Mach Number Flows

Figure 5.7 presents pipe measurements in the form of superficial gas velocity versus void fraction plot. The experimental data is superimposed on the well-known chart for the speed of sound as a function of the void fraction of two-phase mixtures given by Kieffer (1977). Some of the measurements indicate the establishment of the sonic condition. This means that the gas velocities were in the range of subsonic to supersonic conditions. Furthermore, the pressure drop versus superficial gas velocity plots of low liquid rate flows are shown in **Figure 5.8**. The pressure drop increased with superficial gas and liquid velocities. However, at low liquid rates (less than 40 gpm) the pressure drop decreased sharply with gas velocity at high superficial gas velocities. The results indicate the presence of a sonic boundary line in which all the flow curves merge to the line. The reduction in pressure drop was not observed at high superficial liquid velocities (**Figure 5.9**).
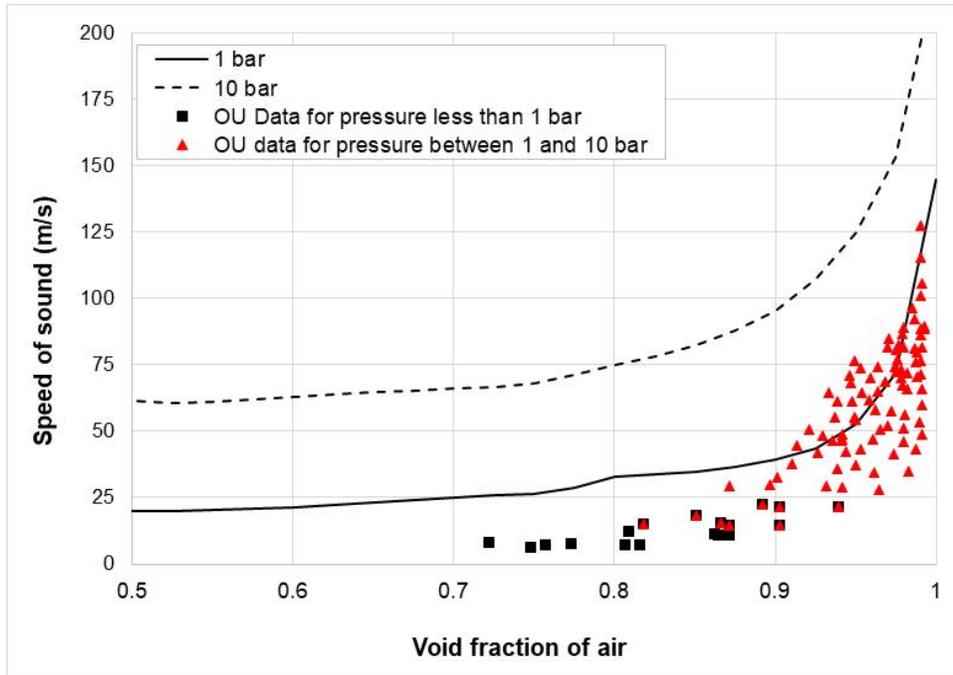
Figure 5.7 High velocity data superimposed on two-phase flow sonic speed (Kieffer, 1977)
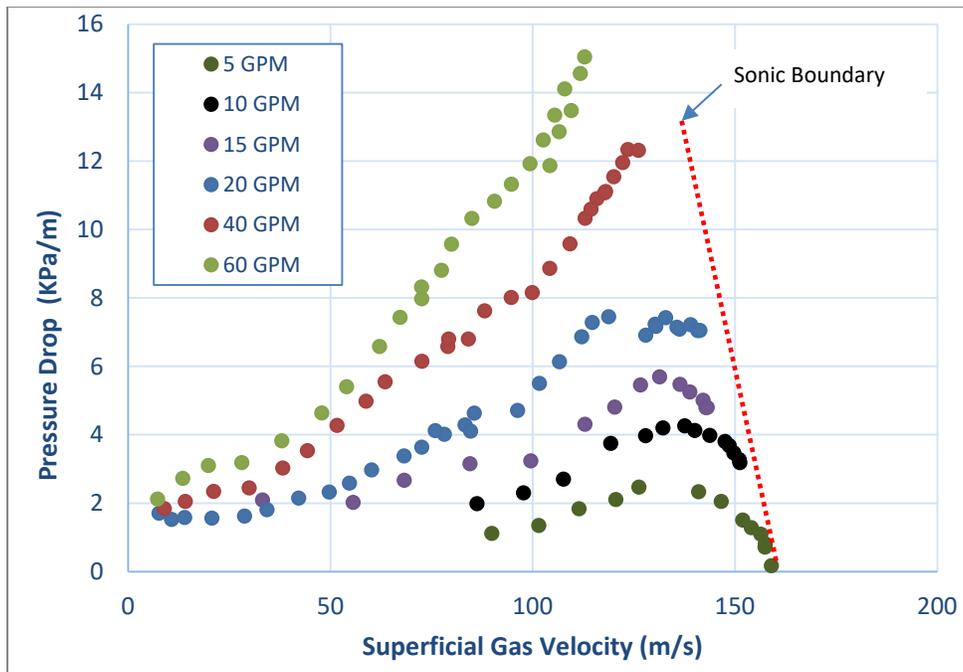
Figure 5.8 Pressure drop vs. superficial gas velocity in pipe at low liquid rates
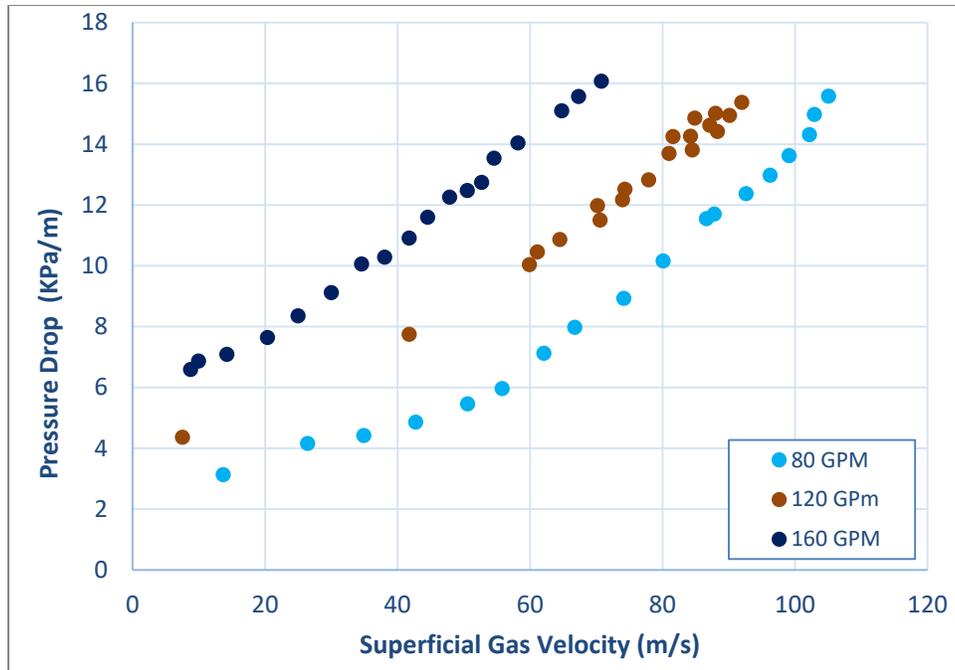
Figure 5.9 Pressure drop vs. superficial gas velocity in pipe at high liquid rates

Figure 5.10 shows the liquid hold up versus superficial gas velocity at different liquid flow rate (superficial liquid velocity). It is worth mentioning that the velocity of gas is calculated based on local density of air. The density of air is calculated using the ideal gas law. The experimental setup has several pressure and temperature sensors installed on the test section. The pressure and temperature sensor measurements in the vicinity of differential pressure cell were utilized for air density calculation. Most of the experimental data reported in the past studies considered the gas phase as incompressible fluid. This assumption is reasonable for low gas velocity experiments. However, at high gas and liquid velocities, the pressure in the test section varies significantly resulting in substantial gas density variation. Hence, the incompressible assumption cannot be valid at high gas and liquid velocities. **Figure 5.11** shows the pressure profiles in the pipe section Vsl of 0.24 m/s and Vsg of 127.4 m/s. The pressure profile in the test section significantly varied at higher velocity. This demonstrates that high Mack number flows need to be treated as compressible flows.
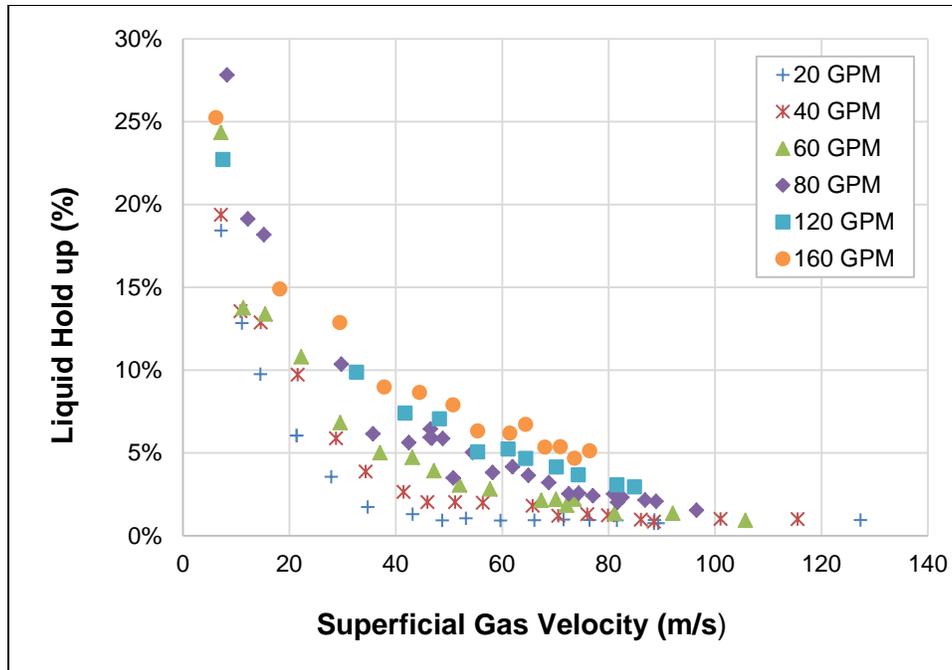
Figure 5.10 Pressure drop vs. superficial gas velocity in pipe at various liquid rates
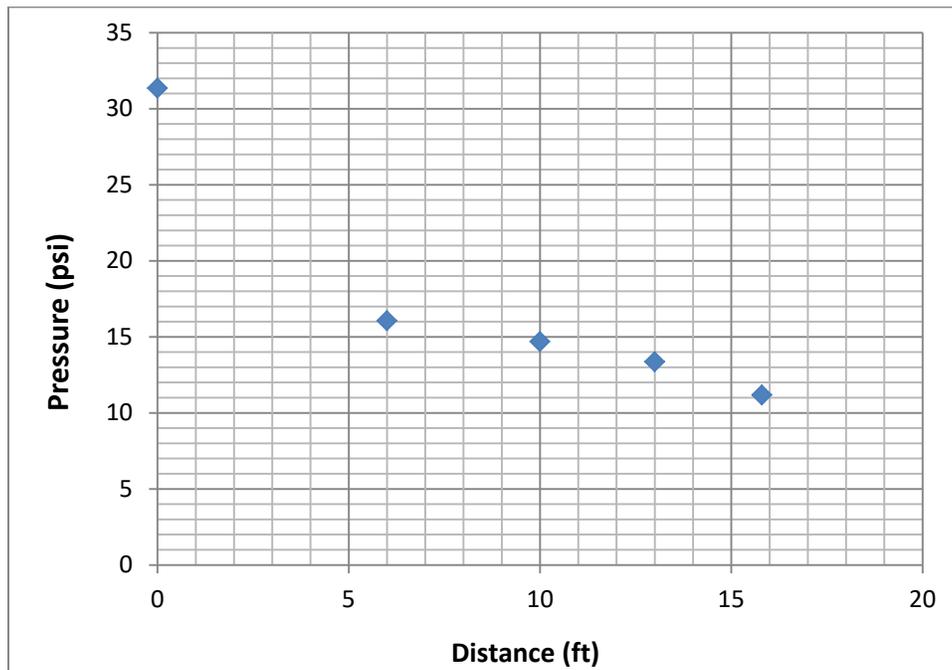
Figure 5.11 Pressure profile in pipe at Vsl of 0.24 m/s and Vsg of 127.4 m/s

One commonly used identification for sonic condition is choking flow in which the fluid velocity becomes independent of the upstream pressure. In order to examine this sonic flow feature, measured upstream pressure is presented as a function of superficial gas velocity (**Figure 5.12**).

For low liquid flow rates, the superficial gas velocity decoupled with the upstream pressure demonstrating the establishment of choking (sonic) flow condition.
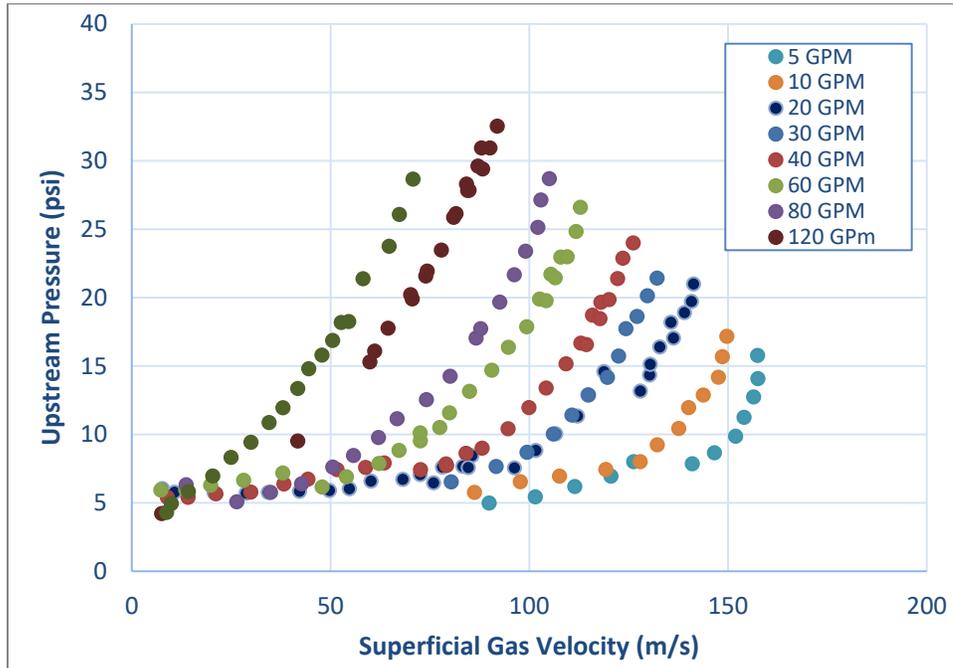
Figure 5.12 Upstream pressure versus superficial gas velocity

5.8 Comparison of Model predictions with Measurements

The need for pressure drop prediction for gas-liquid flow led to the development of a number of empirical and mechanistic models. The experimental pressure drop measurements corresponding to water flow rate of 20 GPM and different superficial gas velocities (7.171 m/s – 66.077 m/s) were compared with Dun and Ros empirical correlation and Hasan and Kabir mechanistic model (**Figure 5.13**). The empirical correlation underestimates the pressure gradient while the mechanistic model overpredicts it. The error in empirical correlation ranges between 60-95 percent while the mechanistic model shows discrepancies ranging from 55 to 300 percent.
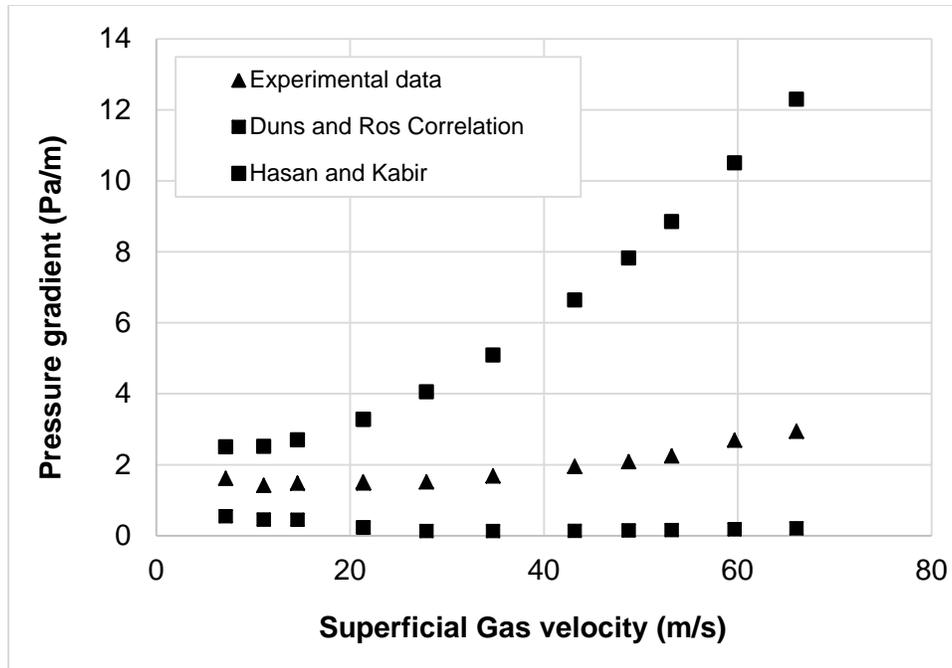
Figure 5.13 Comparison of measured and predicted pressure gradients

6. Two-Phase Flow in Annulus

This section discusses the results of two-phase flow experiments conducted in annulus. Experimental results obtained from the annular section are analyzed considering three important two-phase flow factors (flow regimes, pressure and liquid holdup).

6.1 Flow Regimes in Annulus

The flow regimes in annulus were similar to those observed in vertical pipe. Three flow regimes (churn, transition from churn to annular and annular) were identified in the annulus during the experiments. However, as noted by Caetano (1985), flow pattern characteristics were different from what had been observed in pipe flow. The churn flow in annulus exhibited a distorted Taylor bubble with rising velocity faster than that observed in pipe flow. Annular flow in annulus consists of two liquid films which wet the inner and outer boundary walls (Caetano, 1985). The flow regimes observed in annulus pipe were developed into flow pattern map (**Figure 6.1**). Churn flow regime was observed at high gas velocities. It was a chaotic frothy mixture of gas-liquid moving upward and downward in the entire annulus. During the flow, the liquid film falls down, accumulates, and forms a temporary bridge and lifted upward again by the fast-moving gas. Transition regime is faster and more chaotic when compared to churn. Annular flow regime occurred at high gas and liquid velocities. The liquid film, which flows around the outer pipe-wall was thick and the gas traveled at the core with entrained liquid droplets.
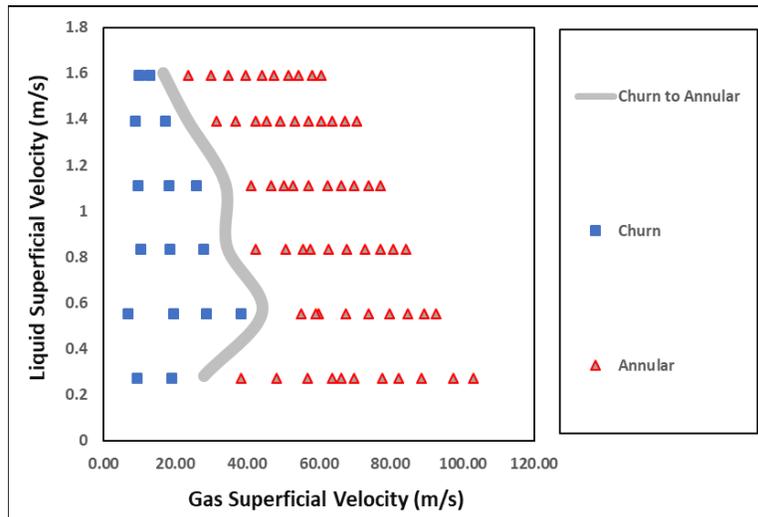
Figure 6.1 Flow regime map for annulus

6.2 Comparison of Flow Regimes in Annulus

The flow patterns observed in annulus are compared with flow patterns map developed by Caetano (1985), which is a modified flow regime map of Taitel and Dukler (1980). The flow patterns observed in this study (churn, churn/annular and annular flow regimes) are imposed on Caetano flow regime map for comparison (**Figure 6.2**). The churn and annular flow regimes from this study are in good agreement with Caetano flow patterns map and data. However, the

transition between churn and annular flow from this study deviate from Caetano's flow pattern map. This could be because of high gas and liquid velocities.
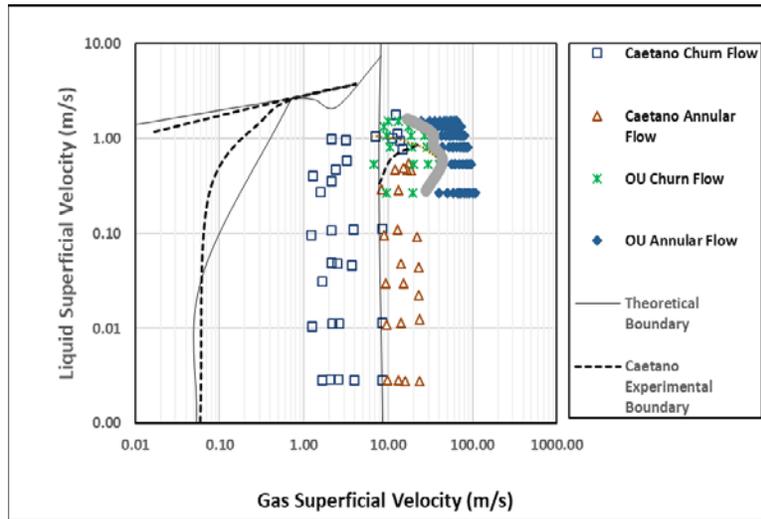
Figure 6.2 Comparison of flow regime using Caetano 1985 flow pattern map

6.3 Liquid Holdup Measurement in Annulus

The liquid holdup trend in the annulus is similar to what was observed in the pipe (**Figure 6.3**). The holdup decreases asymptotically with increasing gas superficial velocity. There is a minor increase in the liquid holdup with liquid superficial velocity.
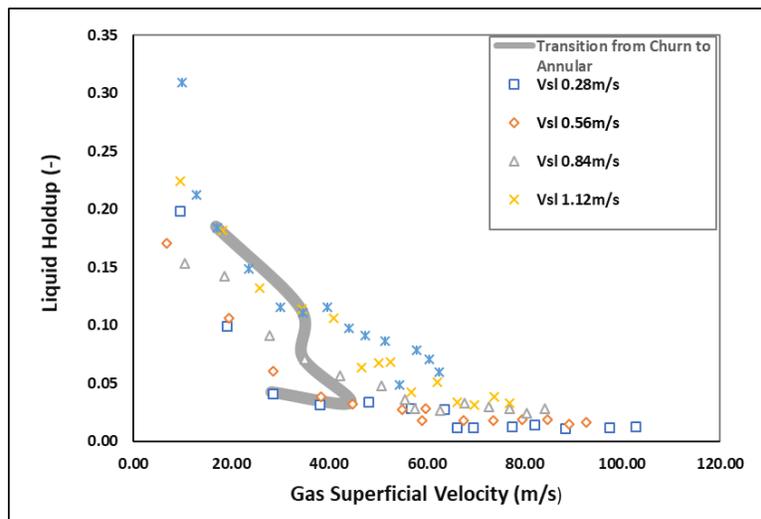
Figure 6.3 Liquid holdup measurements in annulus

6.4 Pressure Gradient in Annulus

The pressure gradient measurements obtained from the annulus have a similar trend as the one obtained from the pipe (**Figure 6.4**). For a given liquid superficial velocity, pressure gradient increased with gas superficial velocity indicating the dominance of friction pressure loss

component of the total pressure drop. Furthermore, at fixed gas superficial velocity, pressure gradient slightly increase with liquid superficial velocity.
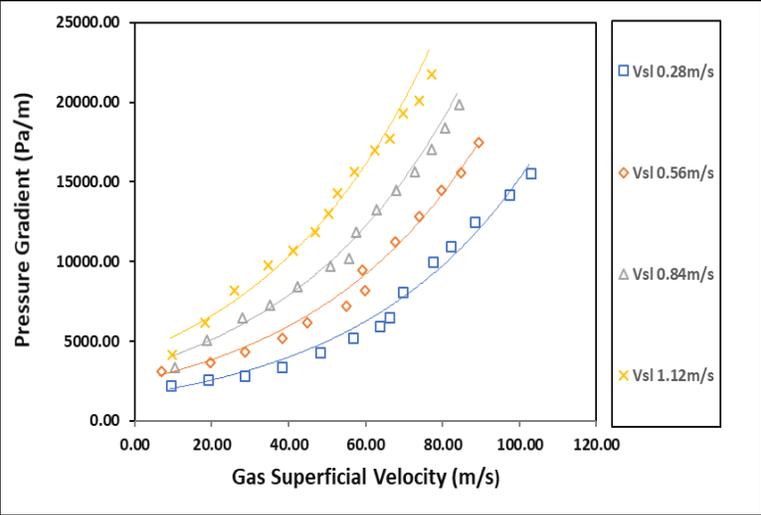
Figure 6.4 Pressure gradient measurements in annulus

7. Conclusion

7.1 Conclusion

The pressure gradient, liquid holdup and flow patterns in gas-liquid two-phase flow have been investigated experimentally in pipe and annulus varying superficial gas and liquid velocities. However, extremely low gas and low liquid velocities were not considered in this study. The outcomes of the investigation are as follows:

- Flow patterns identification and its transition have been an important part of this study. Experiments were carried out to uncover the features of the flow patterns in both pipe and annulus. Visual observation and video recording were employed to identify different flow patterns. Three different flow patterns (churn, annular and transition between churn and annular) were encountered in both pipe and annulus.
- For pipe, pressure drop increased with superficial gas velocities. However, as the flow approaches sonic flow condition, the trend changed and pressure gradient sharply reduced when superficial liquid velocities were low. Reduction in pressure gradient was not observed in the annulus. Moreover, pressure gradient slightly increased with liquid superficial velocity at constant gas superficial velocity. The friction component of the total pressure gradient dominated the two-phase flow hydraulic resistance for both pipe and annular flows.
- In pipe flow, liquid holdup decreased asymptotically with gas superficial velocity.
- In regards to the annulus, similar trends as that of pipe were observed in the liquid holdup measurement. Liquid holdup decreases asymptotically with increasing gas superficial velocity.

References

Ali, S. F. (2009). Two Phase Flow in Large Diameter Vertical Riser. PhD Dissertation. Cranfield University, School of Engineering Department of Process and Systems Engineering

Aliyu, M.A (2015). Vertical annular gas-liquid two-phase flow in large diameter pipes. Ph.D. dissertation, Cranfield University, Cranfied, United Kingdom.

Ansari, M. R. & Azadi, R. (2016). Effect of diameter and axial location on upward gas–liquid two-phase flow patterns in intermediate-scale vertical tubes. Annals of Nuclear Energy, 94 (2016) pp.530–540

Barnea, D., Shoham, O. & Taitel, Y., (1980). Flow pattern characterization in two phase flow by electrical conductance probe. International Journal of Multiphase Flow, 6(5), pp.387–397

Beggs, D. H., & Brill, J. P. (1973). A Study of Two-Phase Flow in Inclined Pipes. Society of Petroleum Engineers. doi:10.2118/4007-PA.

Bourgoyne, A. T., Rocha, L., Bender, C. V., & Bourgoyne, D. 1995. Analysis of Platform Vulnerability to Cratering Induced by a Shallow Gas Flow.

Bowman, S. (2012). Altering an Existing Well Design to Meet New BOEMRE
Worst-Case Discharge Criteria. Society of Petroleum Engineers. doi:10.2118/161929- PA.

Caetano, E. F. (1985). Upward vertical two-phase flow through an annulus. Ph.D. dissertation, The University of Tulsa, Tulsa, Oklahoma.

Caetano, E. F., Shoham, O. O., & Brill, J. P. (1992a). Upward Vertical Two-Phase Flow Through
an Annulus—Part I: Single-Phase Friction Factor, Taylor Bubble Rise Velocity, and Flow Pattern Prediction. ASME. J. Energy Resour. Technol. 1992; 114(1):1-13. doi:10.1115/1.2905917.

Caetano, E. F., Shoham, O. O., & Brill, J. P. 1992b. Upward Vertical Two-Phase Flow through an Annulus—Part II: Modeling Bubble, Slug, and Annular Flow. ASME. J. Energy Resour. Technol. 1992; 114(1):14-30. doi:10.1115/1.2905916.

Cheng, H., HIlls, J. H. & Azzorpardi, B. J. (1998). A study of the bubble-to-slug transition in vertical gas-liquid flow in columns of different diameter. International Journal of Multiphase Flow Vol. 24, No. 3, pp. 431-452.

CSB Report (2014). Explosion and Fire at the Macondo Well. Investigation Report Overview, Volume 2, U.S. Chemical Safety and Hazard Investigation Board. Report No. 2010-10- I-OS

CSB Report (2016). Explosion and Fire at the Macondo Well. Investigation Report Overview, Volume 3, U.S. Chemical Safety and Hazard Investigation Board. Report No. 2010-10-I-OS

Costigan, G. & Whalley, P.B. (1997). Slug flow regime identification from dynamic void fraction measurements in vertical air-water flows. International Journal of Multiphase Flow, 23(2), pp.263–282.

Damir, G. (2012). Multiphase flow in large diameter pipes. M.S. Thesis, University of Nottingham. London, United Kingdom.

Duns, H., & Ros, N. C. J. (1963, January 1). Vertical flow of gas and liquid mixtures in wells. World Petroleum Congress

Fukano,T., & Kariyasaki, A. (1992). Characteristics of gas-liquid two-phase flow in a capillary tube. Nuclear Engineering and Design 141 (1993), pp59-68.

Griffith, P. & Wallis, G.B. (1961). Two-Phase Slug Flow. Journal of Heat Transfer, 83(3), pp.307–318.

Hasan, A. R., & Kabir, C. S. (2007, May 1). A Simple Model for Annular Two-Phase Flow in Wellbores. Society of Petroleum Engineers. doi:10.2118/95523-PA

Hewitt, G., & Hall Taylor, N. (1970). Annular Two-Phase Flow. Pegammon Press, UK.

Jones, O.C. & Zuber, N. (1975). The interrelation between void fraction fluctuations and flow patterns in two-phase flow. International Journal of Multiphase Flow, 2(3), pp.273–306.

Julia, J.E., Ozar, B, Jeong, J., Hibiki, T., & Mamoru Ishii, M. (2011). Flow regime development analysis in adiabatic upward two-phase flow in a vertical annulus. International Journal of Heat and Fluid Flow 32 pp 164–175.

Kieffer, S.W. (1977). Sound speed in liquid-gas mixtures: Water-air and water-steam. Journal of Geophysical research, 82(20), pp.2895-2904.

Lixin, C., Gherhardt, R., & John R.T. (2008).Two-Phase Flow Patterns and Flow-Pattern Maps: Fundamentals and Applications. Transactions of the ASME. 61 pp. 050802-1- 050802-28

 Lucas, D., Krepper, E., & Prasser, H. M., (2005). Development of co-current air–water flow in a vertical pipe. International Journal of Multiphase Flow, 31 (2005) pp.1304–1328.

Matsui, G. (1986). Automatic identification of flow regimes in vertical two-phase flow using differential pressure fluctuations. Nuclear Engineering and Design, 95, pp.221–231.

Matsui, G. (1984). Identification of flow regimes in vertical gas-liquid two-phase flow using differential pressure fluctuations. International Journal of Multiphase Flow, 10 (6), pp.711–719.

McQuillan, K.W., & Whalley, P. B. (1985). Flow Patterns in Vertical Two-Phase Flow. International Journal of Multiphase Flow, 11(2): pp.161-175.

Mishima, K., & Hibiki, T. (1996). Some Characteristics of air-water two-phase flow in small diameter vertical tubes. International Journal of Multiphase Flow, 22 (4), pp. 703-712

Moyer, M. C., Lewis, S. B., Cotton, M. T., & Peroyea, M. (2012, January 1). Challenges Associated with Drilling a Deepwater, Subsalt Exploration Well in the Gulf of Mexico: Hadrian Prospect. Society of Petroleum Engineers. doi:10.2118/154928-MS

Owen, D.G. (1986). An experimental and theoretical analysis of equilibrium annular flows. Ph.D. dissertation, University of Birmgham, United Kingdom.

Ohnuki, A., & Akimoto, H. (1996). An experimental study on developing air-water two-phase flow along a large vertical pipe: Effect of air injection method. International Journal of Multiphase Flow, Vol. 22, No. 6, pp. 1143-1154

Ozar, B., Jeong, J. J., Dixita, A., Juliá, J.E., Hibikia, T., & Ishiia, M. (2008). Flow structure of gas--liquid two-phase flow in an annulus. Chemical Engineering Science 63 (2008) pp 3998-4011

Per Holland. (2017). Loss of Well Control Occurrence and Size Estimators, Phase I and II. BSEE Report no. ES201471/2.

Perez, V. H. (2008). Gas-liquid two-phase flow in inclined pipes. PhD Thesis, University of Nottingham. London, United Kingdom.

Replogle, D.R. (2009). BP: Regional Oil Spill Response Plan - Gulf of Mexico: Appendix Worst Case Discharge. 2009.

Sawai, T., Kaji, M., Kasugai, T., Nakashima, H., & Mori, T. (2004). Gas–liquid interfacial structure and pressure drop characteristics of churn flow. Experimental Thermal and Fluid Science, Vol. 28, pp.597-606.

Shen, X., Saito, Y., Kaichiro Mishima, K., & Nakamura, H. (2006). A study on the characteristics of upward air–water two-phase flow in a large diameter pipe. Experimental Thermal and Fluid Science 31 (2006) pp 21–36

Shen, X., Matsuia, R., Mishimaa, K., & Nakamurab., H. (2010). Distribution parameter and drift velocity for two-phase flow in a large diameter pipe. Nuclear Engineering and Design 240 (2010) pp 3991–4000.

Shipley, D. G. (1984). Shorter Communications: two phase flow in large diameter pipes. Chemical Engineering Science, Volume 39(1), pp. 163-165.

Sun, B., Wang, R., Zhao, X., & Yan, D. (2002). The mechanism for the formation of slug flow in vertical gas–liquid two-phase flow. Solid-State Electronics, 46 (2002) pp.2323–2329.

Szalinski, T., Abdulkaree. L. A., DaSilva, M.J., Thiele, S., Beyer, M., Lucas, D., Perez, H. V., Hampel, U., & Azzopardi. B.J. (2010). Comparative study of gas–oil and gas–water two-phase flow in a vertical pipe. Chemical Engineering Science, 65 (2010) pp.3836–3848

Taitel, Y., Bornea, D. & Dukler, A.E. (1980). Modelling Flow Pattern Transitions for Steady Upward Gas-liquid Flow in Vertical Tubes. AIChE Journal, 26(3), pp.345-354.

Tsoukalas, L.H., Ishii, M. & Mi, Y., (1997). A neuro fuzzy methodology for impedance-based multiphase flow identification. Engineering Applications of Artificial Intelligence, 10(6), pp.545–555.

Tutu, N.K., (1982). Pressure fluctuations and flow pattern recognition in vertical two phase gas liquid flows. International Journal of Multiphase Flow, 8(4), pp.443–447

Vince, M.A. & Lahey, R.T., (1982). On the development of an objective flow regime indicator. International Journal of Multiphase Flow, 8(2), pp.93–124.

Waltrich, P. J., Hughes R., Tyagi M., Kam S., Williams W., Cavalcanti de Sousa P. Zulqarnain M., Lee W., & Capovilla S. M. (2015). Experimental Investigation of Two-Phase Flows in Large-Diameter Pipes and Evaluation of Flow Models Applied to Worst-Case- Discharge

Calculations, BOEM Report M15PC00007, Craft & Hawkins Department of Petroleum Engineering, Louisiana State University, Baton Rouge.

Weisman, J., Duncan, D., Gibson, J., & Crawford, T. (1979). Effects of Fluid Properties and Pipe Diameter on Two-phase Flow Patterns in Horizontal Lines. International Journal of Multiphase Flow, 5(6), pp.437-462.

Zabaras, G., Menon, R., Schoppa, W., & Wicks III, M. 2013. Large Diameter Riser Laboratory Gas-Lift Tests. Offshore Technology Conference, Houston, TX, 6-9 May.

Zangana M., (2011) Film Behaviour of Vertical Gas-Liquid Flow in a Large Diameter Pipe. PhD Thesis, University of Nottingham. London, United Kingdom.

Zubir , M. A., & Zainon, M.Z. (2011). Two-phase flow behavior and patterns in vertical pipe. Journal of Applied Science, 11(9), pp.1491-1500.